RSC Advances

REVIEW

View Article Online
View Journal | View Issue

Cite this: *RSC Adv.*, 2025, **15**, 32080

Diverse chemotypes of polyketides as promising antimicrobial agents: latest progress

Gautam Kumar *[a] and Sidharth Chopra*[bc]

Received 15th May 2025
Accepted 29th August 2025

DOI: 10.1039/d5ra03414k

rsc.li/rsc-advances

Microorganisms, including bacteria, viruses, fungi, and protozoa, significantly impact human health by causing infections that can lead to serious health issues, including mortality and morbidity. Antimicrobials, including antibacterials, anti-virals, anti-fungals, and anti-parasitics, effectively prevent and treat infections in humans and animals. However, pathogens have developed resistance to these antimicrobials, enabling them to survive and persist even in the presence of antibiotics. There is a pressing need to develop new antibiotics with different mechanisms of action to combat infectious diseases effectively. Nature provides a vast therapy and drug discovery resource, offering unparalleled

[a]*Department of Pharmacy, Vidya Vihar, Birla Institute of Technology and Science Pilani, Pilani Campus, Pilani, Rajasthan, 333031, India. E-mail: gautam.kumar@pilani.bits-pilani.ac.in*

[b]*Department of Molecular Microbiology and Immunology, CSIR-Central Drug Research Institute, Sector 10, Janakipuram Extension, Sitapur Road, Lucknow, Uttar Pradesh-226031, India*

[c]*AcSIR: Academy of Scientific and Innovative Research (AcSIR), Ghaziabad, India*

Gautam Kumar

Gautam Kumar is an Assistant Professor at the Department of Pharmacy, Birla Institute of Technology and Science Pilani, Pilani campus, Rajasthan, India. He studied pharmacy during his B. Pharm. and M. Pharm. degrees from Jamia Hamdard, Hamdard University, India. He did his PhD dissertation at the Department of Natural Products, National Institute of Pharmaceutical Education and Research (NIPER) S.A.S Nagar, Punjab, India. During his PhD, he synthesized heterocyclic compounds as potential anti-tubercular agents. He conducted post-doctoral research at the Indian Institute of Technology Bombay, India. During his post-doctoral research work, he was involved in designing and synthesising small bioactive molecules and chemical probes inspired by lipid molecules from Mycobacterium tuberculosis (M.tb), the causative agent of tuberculosis. He has developed "clickable" chemical probes based on M.tb virulence-associated glycolipid, trehalose dimycolate, for real-time proteomics and imaging. Currently, he leads a lab in the area of Natural Products and Medicinal Chemistry at the Department of Pharmacy, Birla Institute of Technology and Science Pilani, Pilani campus, with a focus on bioassay-guided fractionation of extracts, isolation of natural products, phytopharmaceutical formulation development, and synthesis of biologically active molecules.

Sidharth Chopra

Dr. Sidharth Chopra is a Principal Scientist/Associate Professor in the Department of Molecular Microbiology and Immunology at CSIR-Central Drug Research Institute, Lucknow. His research focuses on complementary issues of drug discovery for MDR bacterial pathogens and delineating antimicrobial resistance mechanisms prevalent under Indian conditions. His lab specializes in screening of diverse natural products as well as synthetic organic and inorganic compounds for their antibacterial efficacy from in vitro to animal models of bacterial infections. To better understand the existing and prevalent resistance mechanisms, his lab extensively characterizes clinical isolates at both the genetic and phenotypic level. Together, this data can help guide a more defined approach for successfully identifying molecules with potent activity against MDR pathogens. He completed his PhD from ICGEB/JNU in 2004 with Prof. Anand Ranganathan and moved to Stanford University School of Medicine, Stanford University, USA with Prof. Gary K Schoolnik till 2008. From 2008–12, he was Research Scientist at SRI International, Menlo Park, USA. In 2013, he moved to CSIR-CDRI as Assistant Professor, Department of Microbiology and has established a well funded, vibrant laboratory working on drug discovery targeting MDR bacterial pathogens.

chemical diversity and structural complexity. Among these resources, polyketide synthase machinery produces secondary metabolites in plants, animals, marine organisms, and fungi, significantly contributing to drug discovery. Notably, polyketides exhibit diverse chemotypes, which can facilitate the discovery of antimicrobial drugs. Also, polyketide-based drugs, including anti-bacterial, anti-fungal, and anti-parasitic, have been approved for treating various infectious diseases. This review summarizes recently identified natural polyketides with potential antimicrobial activities.

1. Introduction

An infectious disease is an illness that arises from the presence of a pathogen or the toxins it produces.[1] Microorganisms, including bacteria, viruses, fungi, and protozoa, are responsible for several infections that significantly impact the world by leading to mortality and morbidity.[2] Approximately 30 new causative organisms, mostly of zoonotic origin, have been discovered in recent decades.[3] Tuberculosis (TB), human immunodeficiency virus (HIV), malaria, respiratory tract infections, fungal infections, and diarrheal diseases are among the leading global infections and pose a significant threat to society. Among these, TB is one of the deadliest infections, claiming over 4000 lives daily and remaining the leading cause of death linked to a single pathogen.,[4] 5 Approximately 25% of the worldwide population is latently infected with *Mycobacterium tuberculosis* (*Mtb*).[5] According to the World Health Organization (WHO) report 2023, TB was the second leading cause of death in 2022, following coronavirus (COVID-19).[6] Also, as per the WHO report, an estimated 249 million malaria cases occurred worldwide in 2022.[7] At the same time, fungal pathogens significantly impact global human health and contribute to mortality rates worldwide. Annually, these pathogens are responsible for more than 1.5 million reported cases of infection, affecting over a billion individuals.[8]

The WHO has identified a group of infections caused by ESKAPE (*Enterococcus faecium*, *Staphylococcus aureus*, *Klebsiella pneumoniae*, *Acinetobacter baumannii*, *Pseudomonas aeruginosa*, and *Enterobacter* species) pathogens, which have been given "priority status" due to the urgent need for new antibiotic development. ESKAPE pathogens are also major contributors to the number of deaths caused by infectious diseases.[9] Additionally, the WHO has taken an important step in 2024 by prioritizing the bacterial priority pathogens list. Notably, the WHO has identified 24 bacterial pathogen-drug combinations and classified them based on their assessment outcomes. Based on their impact on the pathogens of the drug, the WHO has categorized bacteria into critical, high, and medium importance. In the critical group category, antibiotic resistance in pathogens poses a significant public health threat due to limited treatment options and a high disease burden associated with mortality and morbidity. This group of bacteria is showing an increasing trend in antibiotic resistance. Few or no promising candidates are in the development pipeline for treating bacteria in the critical group category. Additionally, infections caused by these pathogens are critical; they are challenging to prevent and are highly transmissible. Moreover, these pathogens have exhibited global resistance mechanisms in specific geographical areas.[10]

The antibiotic-resistant pathogens classified as the high group pose significant treatment challenges and contribute to a substantial burden of disease, leading to increased mortality and morbidity in society. This category of bacteria shows a rising trend in resistance, is notably difficult to prevent, and is highly transmissible.[10] A few candidates are in the developmental pipeline for treating these bacterial infections belonging to the high group. While these antibiotic-resistant pathogens may not be considered critical globally, they can be essential to certain populations and specific geographical areas.[10]

In contrast, the antibiotic-resistant pathogens in the medium group are moderately difficult to treat. They cause a moderate burden to society and are responsible for less mortality and morbidity compared to the critical and high groups. Additionally, this group exhibits moderate trends in

Table 1 WHO bacterial priority pathogens list

Critical group	High group	Medium group
Enterobacterales (carbapenem-resistant) Enterobacterales (third-generation cephalosporin-resistant)	*Salmonella typhi* (fluoroquinolone-resistant) *Shigella* spp. (fluoroquinolone-resistant)	Group A Streptococci (macrolide-resistant) *Streptococcus pneumoniae* (macrolide-resistant)
Acinetobacter baumannii (carbapenem-resistant)	*Enterococcus faecium* (vancomycin-resistant)	*Haemophilus influenzae* (ampicillin-resistant)
Mycobacterium tuberculosis (rifampicin-resistant)	*Pseudomonas aeruginosa* (carbapenem-resistant) Non-typhoidal *Salmonella* (fluoroquinolone-resistant) *Neisseria gonorrhoeae* (third-generation cephalosporin and/or fluoroquinolone-resistant) *Staphylococcus aureus* (methicillin-resistant)	Group B Streptococci (penicillin-resistant)

resistance. For this group, relatively more therapeutic candidates are in the developmental pipeline for treatment. These pathogens are critical for certain populations in specific geographical areas.[10] The WHO priority pathogen list 2024 is given in Table 1. Meanwhile, antimicrobial resistance significantly threatens all medical and public health aspects. It undermines the control of infectious diseases by increasing morbidity and mortality while imposing substantial costs on society.[11] Thus, a crucial unmet need exists to identify novel molecules for treating microbial diseases.

2. Polyketides as diverse scaffolds with immense medicinal value

The chemical synthesis of diverse chemotypes of compounds remains challenging. Additionally, exploring novel natural compounds for potential antimicrobial activities has been demanding. Polyketides represent one of the most significant classes of natural products in drug discovery, particularly for antimicrobial development.[12–14] These structurally diverse secondary metabolites are produced mainly by bacteria, fungi, and plants through the polyketide synthase (PKS) pathway, serving as a treasure trove for drug discovery. Their importance in antimicrobial drug discovery stems from their potent biological activities, structural versatility, and ability to target a wide range of pathogens. Polyketides are of several classes of compounds, including benzophenone analogues, dihydrobenzofurans, isocoumarins, chromone derivatives, xanthones, anthraquinones, aromatics, macrolides, polyenes, and polyethers.[15] The diverse scaffolds produced by the PKS machinery make them a center of research attraction for drug discovery and development.[16] Many polyketides exhibit strong antimicrobial properties against Gram-positive and Gram-negative bacteria, fungi, and parasites. For example, erythromycin displays a broad spectrum of antibacterial activity against Gram-positive bacteria, while tylosin and spiramycin are macrolide-based polyketides with antibacterial activity.[12–14] At the same time, amphotericin B is a polyene-based polyketide that acts as an anti-fungal and anti-leishmanial agent. One of the most compelling aspects of polyketide antimicrobials is that they often possess unique modes of action.[13,17]

Polyketides are biosynthesized from the acyl-CoA or malonyl-CoA precursors and catalyzed by the PKS enzyme complex. The PKS enzyme complex consists of ketosynthase, acyltransferase, and acyl carrier protein (ACP), which catalyzes polyketide chain elongation. Polyketide biosynthesis is a complex process; a ketosynthase facilitates the Claisen condensation of activated acyl and malonyl building blocks. An acyltransferase selects the loading extender units, while an acyl carrier protein domain anchors the growing chain.[16] Additionally, some of the PKS enzyme complexes also contain ketoreductase (KR), dehydratase (DH), and enoylreductase (ER) domains. In the polyketide synthesis process, a ketoreductase stereospecifically reduces the β-keto group, a dehydratase removes water from the resulting β-hydroxy group, and an enoylreductase reduces the β-carbon to form a methylene group. A thioesterase located at the C-terminus of these synthases effectively facilitates the release of the final product (polyketide) through hydrolysis or cyclization.[18]

2.1. An overview of FDA-approved polyketide-based drugs

To date, several polyketide-based drugs have been approved for treating infectious, parasitic, and metabolic disorders. For instance, rapamycin (**1**, Fig. 1) is a macrocyclic polyketide biosynthesized by various actinomycetes, including *Streptomyces hygroscopicus*, *Streptomyces iranensis*, and *Actinoplanes* sp. N902-109 is approved as an immunosuppressant for patients receiving solid organ transplants. Additionally, rapamycin exhibits antifungal activity, anticancer activity, and neuroprotective and neurogenerative properties.[19] Meanwhile, the compound tacrolimus (**2**, Fig. 1) and its semi-synthetic derivative FK-520 are used in organ transplants to treat autoimmune diseases.[20]

Lovastatin (**3**, Fig. 1) was first isolated from *Monascus ruber*. It reduces endogenous lipid synthesis and the absorption of exogenous lipids, promoting their transport and excretion. It inhibits cholesterol biosynthesis by competitively inhibiting HMG-CoA (3-hydroxy-3-methylglutaryl-coenzyme A) reductase, thus lowering blood lipid levels. Recent studies suggest that lovastatin prevents acute myeloid leukemia, colon, breast, liver, cervical, and lung cancer.[21] Additionally, lovastatin is found to be useful in neurological disorders, including Parkinson's disease and type I neurofibromatosis.[22] Vibralactones are produced by the basidiomycete fungus *Boreostereum vibrans*, a potential pancreatic lipase inhibitor.[23]

Avermectins are a large group of structurally similar 16-membered macrolactones comprising uncommon spiroacetal and tetrahydrofuran moieties produced from the fermentation of *Streptomyces avermitilis.* Various avermectin derivatives, differing in substitution patterns, are produced by multimodular polyketide and accessory enzymes.[24] Naturally occurring avermectins comprise a mixture of four distinct compounds: avermectin A1 (**4**, Fig. 1), A2 (**5**, Fig. 1), B1 (**6**, Fig. 1), and B2 (**7**, Fig. 1). Each of these compounds has two variants, designated as a and b. The filarial worm, *Onchocerca volvulus*, causes river blindness (onchocerciasis), and worm infection in the lymph leads to lymphatic filariasis. These compounds are widely used in medicine for their anthelmintic properties. Ivermectin is most commonly used as an antiparasitic in livestock, pets, and humans.[25] Ivermectin significantly affects the motility, feeding, and reproduction of nematodes, primarily by blocking the glutamate-gated chloride channel. Chloride channels are common in nematode neurons and pharyngeal muscle cells, leading to the easy paralysis of the parasite.[25,26] Moreover, ivermectin is also used to treat onchocerciasis and lymphatic filariasis. A recent study found that ivermectin, selamectin, and moxidectin displayed activity against *Mtb*.[27]

Erythromycin (**8**, Fig. 1) consists of a 14-membered lactone, erythronolide B, which includes two deoxysugars: L-mycarose and α-D-desosamine. It exhibits broad-spectrum activity against both Gram-positive and Gram-negative bacteria. Erythromycin

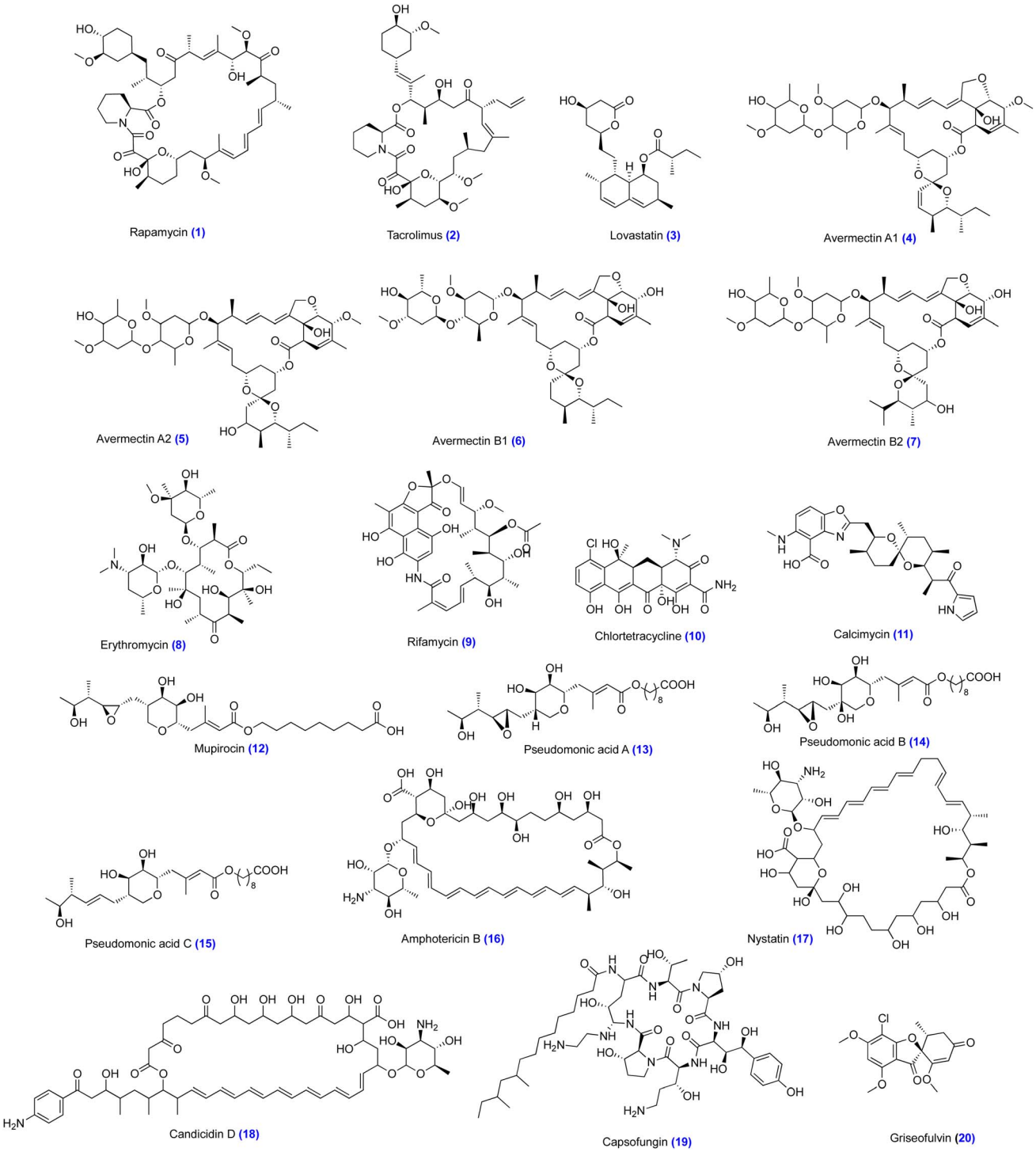

Fig. 1 Chemical structures of FDA-approved polyketide-based drugs.

interacts with the 50s ribosomal subunit of prokaryotic ribosomes, inhibiting protein synthesis. However, it suffers from acid instability. Rifamycin (**9**, Fig. 1) is derived from the soil bacteria *Amycolatopsis mediterranei* or *Amycolatopsis rifamycinica*.[28] Rifampicin binds to the β-subunit of DNA-dependent RNA polymerase, inhibiting RNA synthesis. The four hydroxyl groups of rifampicin contribute to forming the ansa bridge. Additionally, the hydroxyl groups of the naphthol ring establish hydrogen bonds with amino acids in RNA polymerase. The binding of rifampicin to the DNA/RNA channel of the β-subunit of RNA polymerase obstructs RNA elongation, truncating RNA transcripts, and inhibiting bacterial protein synthesis.[29]

In the tetracycline class, the first antibiotic, 6-chlorotetracycline (**10**, Fig. 1), was identified and isolated from the bacterium *Streptomyces aureofaciens*.[30] It showed broad-spectrum activity against Gram-positive and Gram-negative

bacteria, spirochetes, obligate intracellular bacteria, and protozoan parasites. Tetracyclines specifically bind to bacterial ribosomes, interacting with a highly conserved 16 s ribosomal RNA (rRNA) target in the 30s ribosomal subunit. This process halts translation by interfering with the attachment of aminoacyl-tRNA during elongation.[31]

Calcimycin (**11**, Fig. 1) was isolated from *Streptomyces chartreusensis*. Calcimycin is an ionophore that transports divalent cations, including calcium and magnesium. It exhibits antimicrobial activity against Gram-positive bacteria and fungi. A recent study demonstrated that it mediates the mycobacterial killing of *Mycobacterium bovis* BCG *in vitro* and in THP-1 cells by inducing calcium-regulated autophagy in a P2RX7-dependent manner.[32] Another study suggests that it mediates apoptosis in breast and cervical cancer cell lines by increasing the intracellular calcium level and the expression of the ligand-gated channel P2RX4.[33]

Mupirocin (**12**, Fig. 1) is obtained from *Pseudomonas fluorescens*. Notably, it has a unique chemical structure comprising a mixture of several pseudomonic acids A, B, and C (**13–15**, Fig. 1); among them, pseudomonic acid A constitutes more than 90%.[34] It displays antibacterial activity by binding to the leucine-specific tRNA aminoacyl synthetase enzyme, thereby interfering with protein synthesis. Mupirocin is used for treating skin infections caused by *S. aureus*.[35]

In the antifungal category, amphotericin B (**16**, Fig. 1), nystatin (**17**, Fig. 1), and candicidin D (**18**, Fig. 1) are polyene macrolide polyketides that display broad-spectrum antifungal activity. The polyene macrolide antibiotics typically feature a large macrocyclic lactone ring with a conjugated double-bond system and are generally associated with hydrophilic substituent iminosugars.[36] Amphotericin B and nystatin target ergosterol in the plasma and vacuole membranes. They also induce ion channel formation and cause leakage of the membrane functions, thereby killing the cells.[37] Recent studies suggest that nystatin eliminates biofilm formation in *Candida albicans* and *Streptococcus mutans.*[38] In contrast, caspofungin (**19**, Fig. 1) is a non-ribosomal polyketide that exhibits antifungal activity by acting on β-1,3-glucan synthase and hindering the biogenesis of the fungal cell wall. *Griseofulvin* (**20**, Fig. 1) is a spirocyclic benzofuran-3-one produced by *Penicillium griseofulvum*. It is an oral antifungal drug that treats dermatomycoses, including ringworm and tinea pedis. Griseofulvin exhibits antifungal activity by binding to microtubules and inhibiting mitosis.[39]

3. Polyketide-based leads as antibacterial

Antimicrobials, including antibacterials, antivirals, antifungals, and antiparasitics, are essential drugs that effectively prevent and treat infections in humans, animals, and plants. However, the development of antimicrobial resistance (AMR) in pathogens allows them to persist and survive in the presence of antimicrobial drugs.[40] Bacteria have evolved several robust mechanisms to evade antimicrobials' effects efficiently. These molecular strategies for antimicrobial resistance include active efflux systems that pump antimicrobial agents out of bacterial cells, modifications to the bacterial membrane that block the entry of these agents, and changes to the target sites that prevent the binding of antibiotics. Furthermore, the enzymatic breakdown of antimicrobial substances renders them ineffective. Additionally, thick biofilms form a formidable barrier around bacterial cells. These mechanisms (Fig. 2) not only enhance bacterial survival but also significantly challenge the effectiveness of antimicrobial treatments.[41]

Macrobrevins were first isolated from *Brevibacillus* sp. associated with *Arabidopsis thaliana* phyllosphere. In a study, Chakraborty *et al.* investigated the biosynthetic potential of *Bacillus amyloliquefaciens* MTCC 12713, which was isolated from the intertidal macroalga *Kappaphycus alvarezii* (Doty) L.M. Liao. Notably, *Bacillus amyloliquefaciens* extracts exhibited antibacterial activity against methicillin-resistant *Staphylococcus aureus* (MRSA) and vancomycin-resistant *Enterococcus faecalis* (VRE). Further, the bioassay-guided fractions led to the isolation of polyketides (**21–24**, Fig. 3) that showed antibacterial activity against MRSA, VRE, *Klebsiella pneumoniae*, and *Pseudomonas aeruginosa*, with minimum inhibitory concentration (MIC) ranging from 1.56–6.25 μg mL^{-1} and against these strains, chloramphenicol exhibited MIC of 6.25–12.5 μg mL^{-1}, respectively. Further, *in silico* studies confirmed that macrobrevins showed antibacterial activity by binding to *S. aureus* peptide deformylase.[44]

Zaman *et al.* isolated three polyketides (**25–27**, Fig. 3) from the fungal strain *Fusarium graminearum* FM1010 and assessed their antibacterial *activity against S. aureus*. The isolated polyketides demonstrated moderate antibacterial activity against *S. aureus*, with MIC values of 80, 80, and 160 μg mL^{-1}, respectively. Additionally, **25–27** modulated the activity of chloramphenicol against *S. aureus*. Next, compounds **25–27** were evaluated against human embryonic kidney cells 293 (HEK 293) at 50 μM, and these compounds were non-toxic to the HEK 293 cells. However, **27** inhibits A2780 human ovarian cancer cells with a moderate IC_{50} value of 18.52 μM, which might limit its development as an antibacterial agent.[45]

Tetracenomycin structures (**28–34**, Fig. 3) are similar to tetracycline, a well-known translation inhibitor. Tetracenomycin is a potent inhibitor of protein synthesis that does not damage DNA. Interestingly, tetracenomycin does not interact with the smaller ribosomal subunit; instead, it binds to the larger ribosomal subunit, specifically within the polypeptide exit channel (Fig. 4). The binding site for tetracenomycins is adjacent to the macrolide binding site, where TcmX stacks on the noncanonical base pair formed by U1782 and U2586 of the 23S ribosomal RNA, effectively blocking protein translation.[46] Alferova *et al.* isolated the tetracenomycins congener O^4–Me-tetracenomycin C from *Amycolatopsis* sp. strain A23, which showed antibacterial activity against *E. coli* with a MIC of 16 μg mL^{-1}. In contrast, erythromycin, tetracenomycin C (**31**), and tetracenomycin X (**32**) inhibited *E. coli* with the same MIC of 2 μg mL^{-1}. Tetracenomycin exhibits antibacterial activity by blocking protein synthesis and inhibiting ribosomal activity. However, compound O^4–Me-tetracenomycin C (**34**) could not inhibit the ribosome, as it is substituted with methoxy at the 4th position, confirming that the hydroxyl group is crucial for binding at the ribosome.[47]

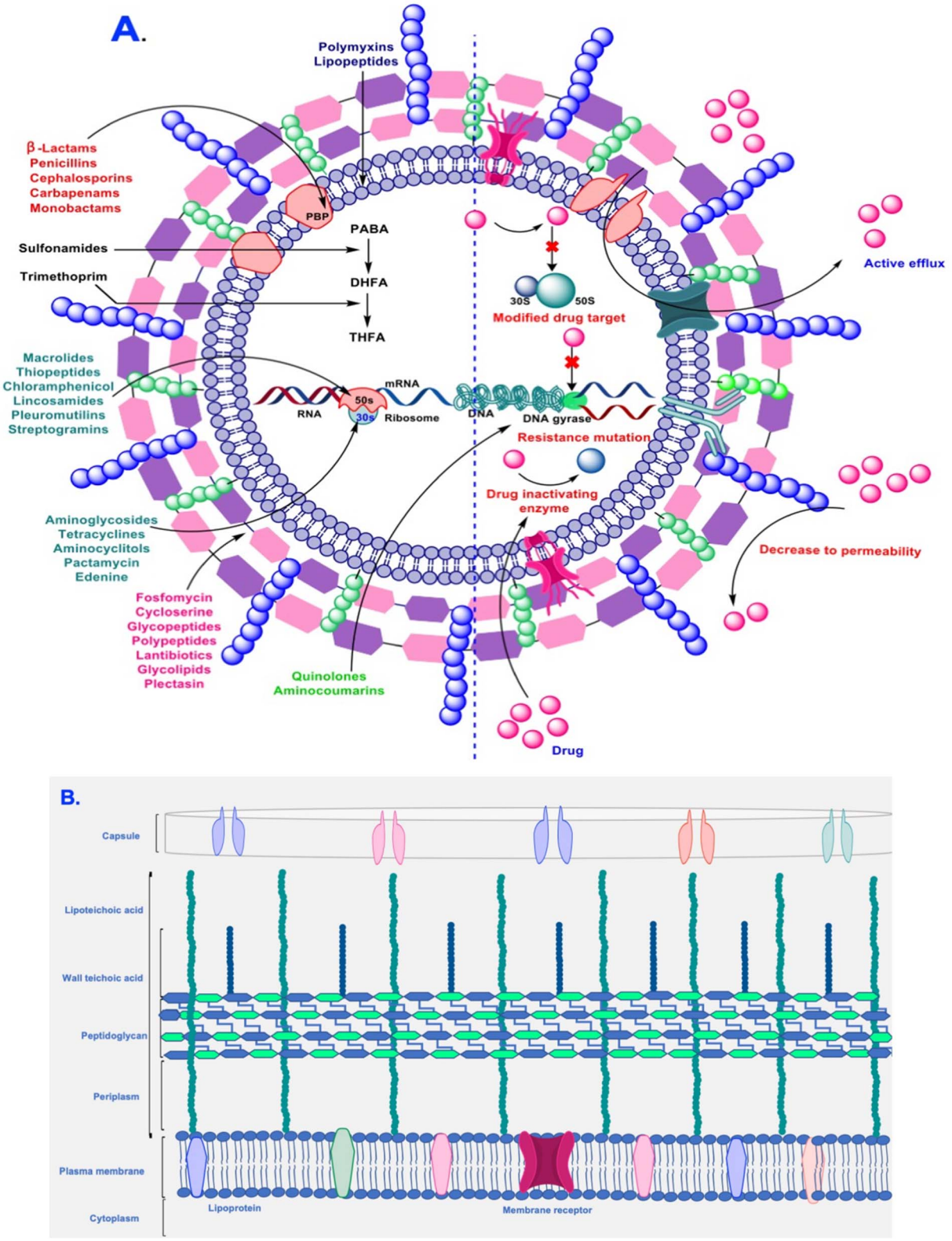

Fig. 2 (A) A pictorial representation depicting Gram-positive (*S. aureus*) targets and molecular strategies developed by bacteria to avoid antimicrobials. (B) A diagrammatic representation illustrating the Gram-positive membrane.[42,43]

The erythromycin TMC-154 (**35**, Fig. 3) is an antibacterial compound derived from the rhizospheric fungus *Clonostachys rogersoniana*, which associates with the *Panax notoginseng*. TMC-154 exhibited antibacterial activity against *S. aureus*, *S. pyogenes*, *S. mutans*, *P. aeruginosa*, and *V. parahaemolyticus*, with MIC_s of 125, 25, 25, 62.5, and 62.5 μM, respectively. TMC-145

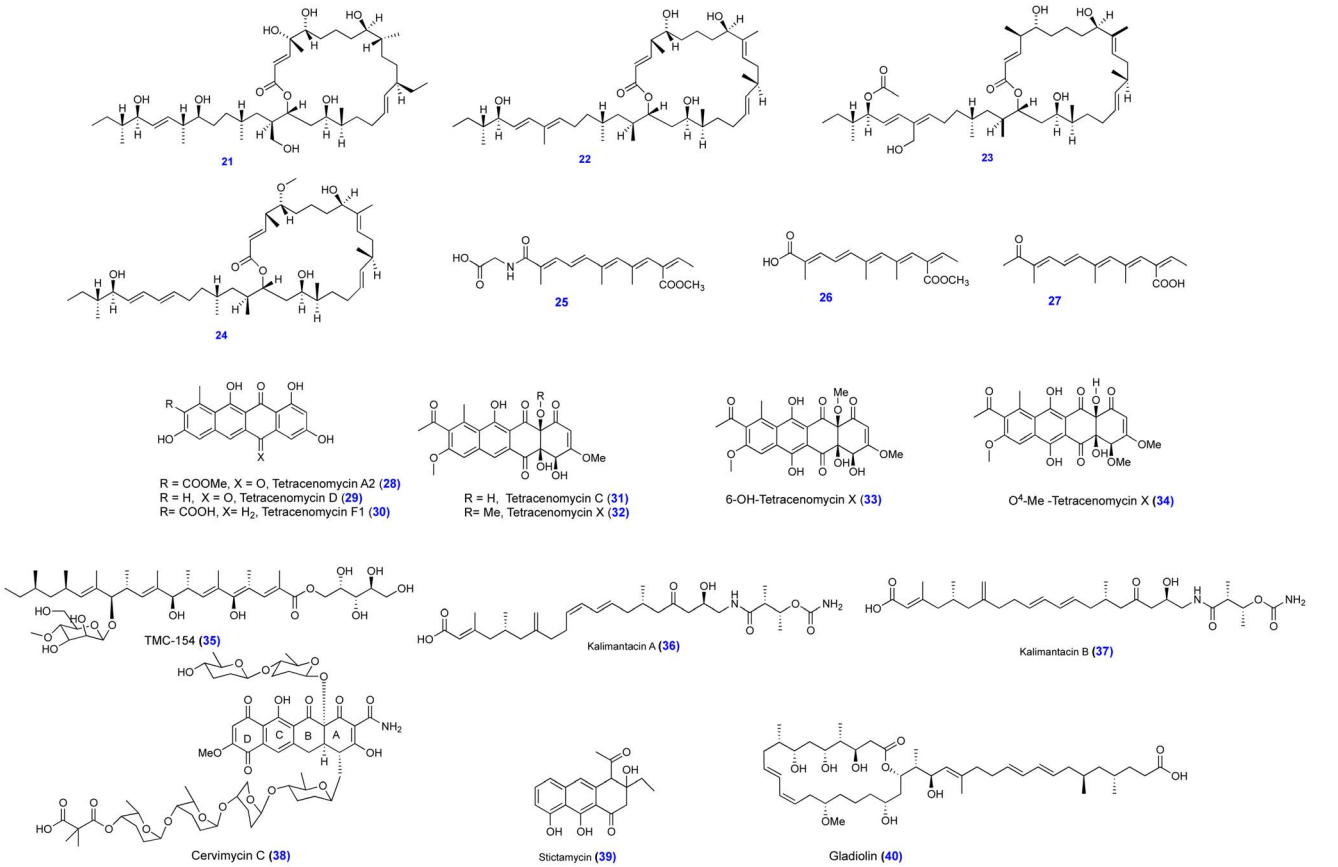

Fig. 3 Chemical structures of polyketide-based compounds (**21–40**) as antibacterial agents.

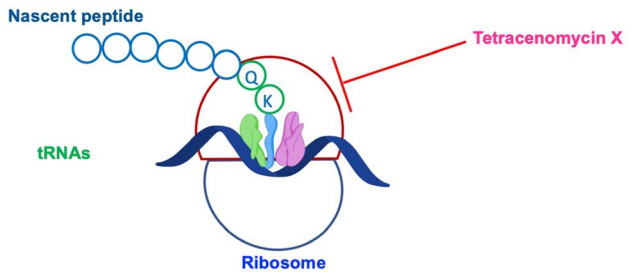

Fig. 4 A diagrammatic representation depicting tetracenomycin X inhibits peptide bond formation between an incoming aminoacyl-tRNA and a terminal Gln–Lys (QK) motif in the nascent polypeptide.

exerts antibacterial activity by generating reactive species (RS) within *S. pyogenes*. Additionally, TMC-154 demonstrated synergistic activity with well-known antibiotics, including ciprofloxacin and chloramphenicol, against *S. pyogenes*.[48]

Kalimantacin A, or batumin (**36**, Fig. 3), was isolated from *Alcaligenes* sp. YL-02632S and *Pseudomonas fluorescens*. It is biosynthesized by a hybrid type I *trans*-acyltransferase (AT), polyketide synthase (PKS), and non-ribosomal peptide synthase (NRPS). It demonstrated antibacterial activity against *Staphylococcus* species. Kalimantacin B is the E, E-diene isomer of kalimantacin A, isolated from *Alcaligenes* sp. YL-02632S. Kalimantan B (**37**, Fig. 3) was found to be four to eight-fold less potent than Kalimantan A. Notably, Kalimantan A showed antibacterial activity against *S. aureus* by inhibiting fatty acid synthase activity through binding to FabI (Fig. 5). Kalimantacin A inhibits *S. aureus* ATCC 6538 and *S. aureus* RN4220 at the same MIC of 0.125 μg mL^{-1}.[49,50]

Cervimycins A-D are bis-glycosylated polyketides biosynthesized by *Streptomyces tendae* HKI 0179. They exhibit bactericidal activity against Gram-positive bacteria. Cervimycins C (**38**, Fig. 3) inhibit *B. subtilis* 168 and *S. aureus* SG511 Berlin, with MICs of 0.25 and 2 mg L^{-1}, whereas cervimycins D inhibit the same bacteria with MICs of 0.5 and 32 mg L^{-1}, respectively. Moreover, *Bacillus subtilis* 168 treated with cervimycin C exhibited spaghetti-like phenotypic characteristics with elongated, curved cells that resulted in ghost cells without DNA. Furthermore, electron microscopy of cervimycins C-treated *S. aureus* revealed swollen cells, thickening with rough cell surfaces, and misshapen septa. At low concentrations, cervimycins C act on DNA. Moreover, cervimycin C stimulated the expression of the CtsR/HrcA heat shock operon and the expression of autolysins, revealing a similarity to gentamicin.[51]

Hou *et al.* isolated stictamycin (**39**, Fig. 3) from the organic extracts of *Streptomyces* sp. 438-3, an isolate from the New Zealand lichen *Sticta Felix*. Stictamycin demonstrated antibacterial activity against *B. subtilis* E168, *E. coli* (TolC-deficient), and *S. aureus*, with MIC of 32, 32, and 2 μg mL^{-1}, respectively.[52]

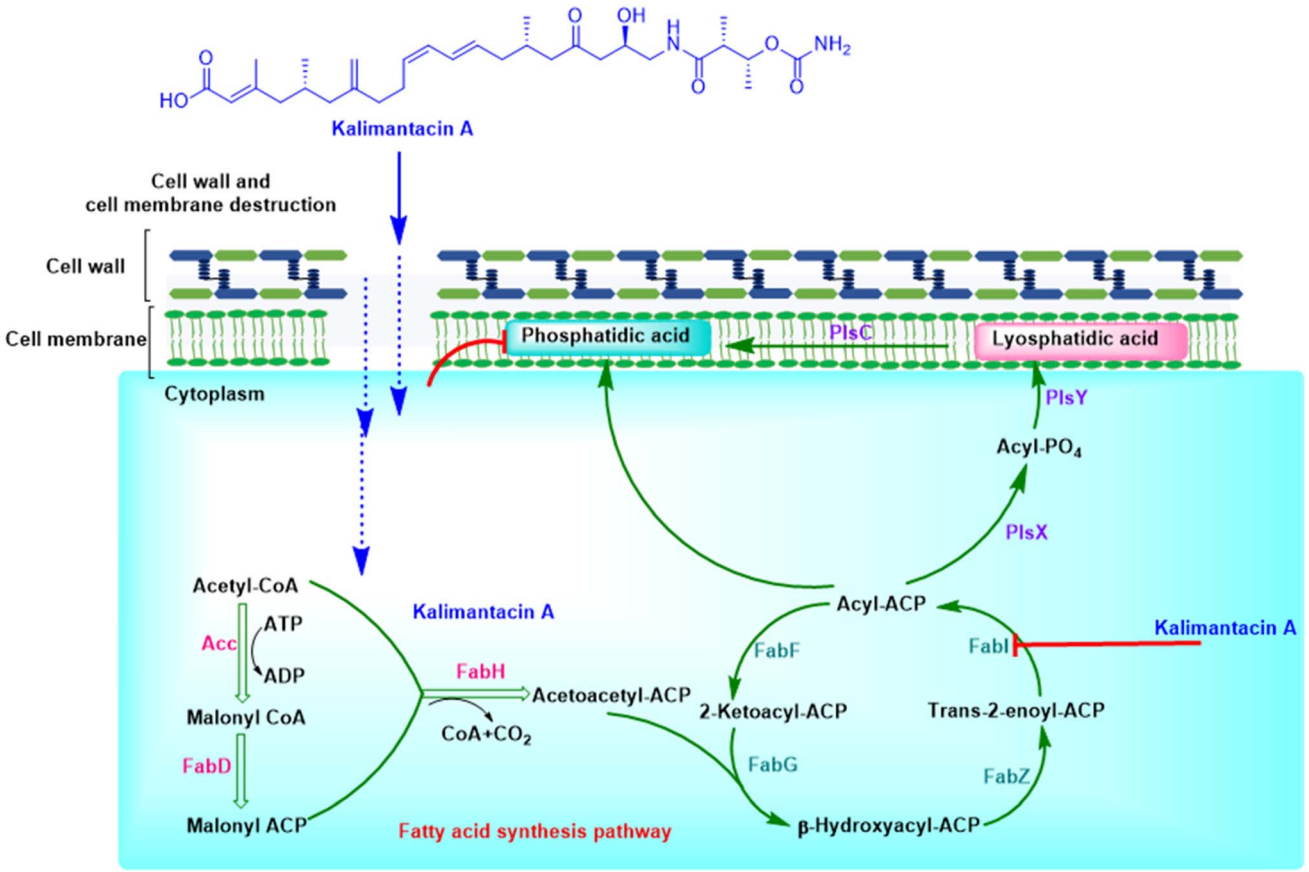

Fig. 5 A pictorial representation of the biosynthetic pathway in *S. aureus*. Kalimantacin A exhibits antibacterial activity by inhibiting FabI of the fatty acid biosynthetic pathway.[57]

Gladiolin (**40**, Fig. 3) was isolated from *Burkholderia gladioli* and has a structural resemblance to another polyketide, etnangien. Due to its shorter and more saturated C21 side chain, it exhibits greater acid and light stability than etnangien.[53] It demonstrated promising antibacterial activity against clinical isolates of *Mtb* and *Neisseria gonorrhoeae*.[50,54] The cellular target of gladiolin is bacterial RNA polymerase, resulting in the inhibition of transcription.[55] A study by Simm *et al.* has shown that gladiolin synergizes with the activity of amphotericin B and enhances its effectiveness against *Cryptococcus* and *Candida* species, including drug-resistant *C. auris*. Gladiolin interacts with the bacterial membrane, modulating the binding mode of amphotericin B and causing membrane thinning by decreasing ergosterol content, pore formation, and increased membrane destruction.[56]

Liu *et al.* isolated argenteolides A (**41**, Fig. 6) and B (**42**, Fig. 6), glycosylated polyketide-peptide hybrid macrolides from *Streptomyces argenteus*. Compounds **41** and **42** inhibited *S. aureus* and *Escherichia coli* ATCC25922, with MICs of 11.6, 21.0, and 15.7, 27.9 μg mL^{-1}, respectively. Additionally, argenteolides A (**41**) and B (**42**) demonstrated cytotoxicity to A549, P388, and HeLa cell lines with IC_{50} values of 28.8 and 46.5 μM, and 31.5 and 40.8 μM, 25.2 and 37.5 μM, respectively. The cytotoxicity of compounds **41** and **42** might limit their development as antibiotics.[58]

Diaphorin (**43**, Fig. 6) is biosynthesized by *Candidatus profftella* armature, an obligate symbiont of the Asian citrus psyllid *Diaphorina citri*. Diaphorin is known for its inhibitory activity against several eukaryotes. A study performed by Tanabe *et al.* has demonstrated that diaphorin inhibits the growth and cell division of *Bacillus subtilis*. However, it promotes the growth and metabolic activity of *E. coli*.[59]

The *Bacillus amyloliquefaciens* MTCC12713 is associated with the intertidal macroalga *Kappaphycus alverezii*. The *Bacillus amyloliquefaciens* displayed antibacterial activity against multidrug-resistant Gram-positive bacteria. Further genome mining and bioassay-guided fractionation led to the isolation of the compound difficidin and its analogues (**44–47**, Fig. 6). Notably, these analogues demonstrated bactericidal activity against vancomycin-resistant *Enterococcus faecalis*, MRSA, *Klebsiella pneumoniae*, and *Pseudomonas aeruginosa*, with the MIC ranging from 2–9 × 10^{-3} μM. These analogues exhibited more potent antibacterial activity compared to the standard drugs, chloramphenicol and ampicillin.[60] Further, the bioassay-guided fraction of the *Bacillus amyloliquefaciens* MTCC12713 led to the identification of the bacillibactins class of siderophores (**48–51**, Fig. 6). These compounds exhibited bactericidal activity against multidrug-resistant strains, including *Escherichia coli*, *V. parahaemolyticus*, *P. aeruginosa*, *K. pneumoniae*, *E. tarda*, *S. pyogenes*, MRSA, and VREs, with MIC ranging from 1.56–6.25 μg

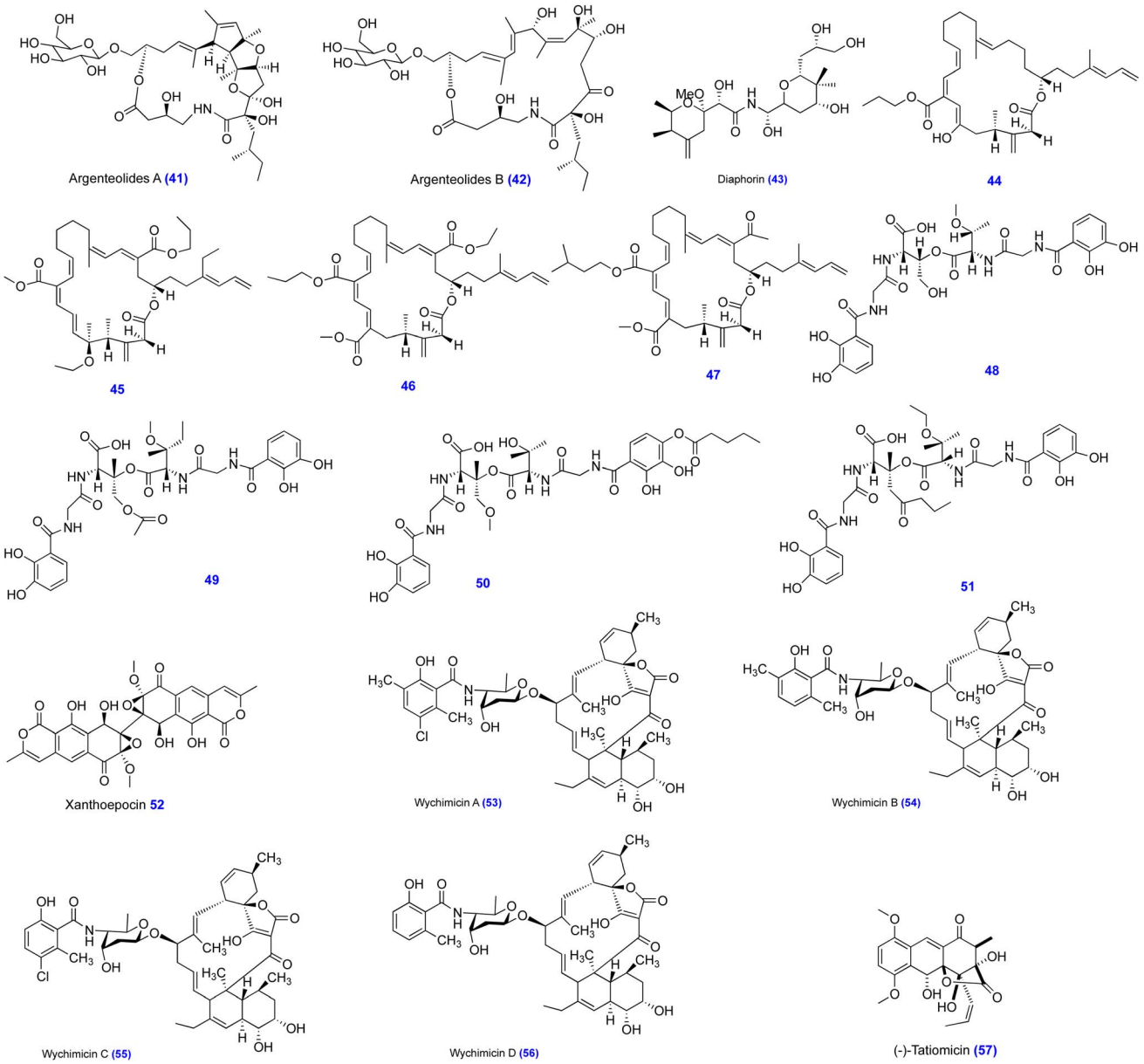

Fig. 6 Chemical structures of polyketide-based compounds (41–57) as antibacterial agents.

mL^{-1}. In contrast, the standard chloramphenicol showed antibacterial activity against the same bacterial strains, with MICs ranging from 6.25 to 12.5 μg mL^{-1}, respectively. The structure–activity relationship (SAR) revealed that compounds with higher electronic values possess greater antibacterial potential.[61]

Xanthoepocin (**52**, Fig. 6) is a polyketide antibiotic biosynthesized by *Penicillium ochrochloron*. Vrabl *et al.* demonstrated that xanthoepocin is a photolabile compound that produces singlet oxygen under blue light irradiation. Interestingly, xanthoepocin exhibited antibacterial activity against MRSA with light protection measures, showing MIC values up to 5 times lower than previously reported. It was also highly active against clinical isolates resistant to linezolid and VRE.[62]

Kimura *et al.* have identified 13-membered macrocyclic spirotetronates with a *trans*-decalin glycoside moiety, termed wychimicins A-D (**53–56**, Fig. 6), from the culture broth of the *Actinocrispum wychmicini* strain MI503-AF4. Wychimicins A-D demonstrated antibacterial activity against *S. aureus*, *Bacillus cereus*, *Corynebacterium bovis*, *Enterococcus faecalis*, and *Enterococcus faecium.*[63]

Kepplinger *et al.* has identified an antibiotic (−)-tatiomicin (**57**, Fig. 6), from an extremophile *Amycolatopsis* sp. DEM30355 using genomic and bioactivity-informed analysis. (−)-tatiomicin displayed no detectable antimicrobial activity against Gram-negative bacteria and *Candida* spp. Notably, it showed antibacterial activity against *Staphylococcus* and *Streptococcus* species, with the MIC of 4–8 μg mL^{-1}. *B. subtilis* 168CA-CRW419 treated with (−)-tatiomicin exhibited chromosome

decondensation, and the effects were similar to those of rifampicin. Furthermore, single-cell microscopy suggested that (−)-tatiomicin causes membrane depolarisation in bacteria.[64]

Wu *et al.* identified macrocyclic spirotetronate polyketide glenthmycins A-M (**58–70**, Fig. 7) from Australian pasture plant-derived *Streptomyces* sp. CMB-PB041. Glenthmycins and their

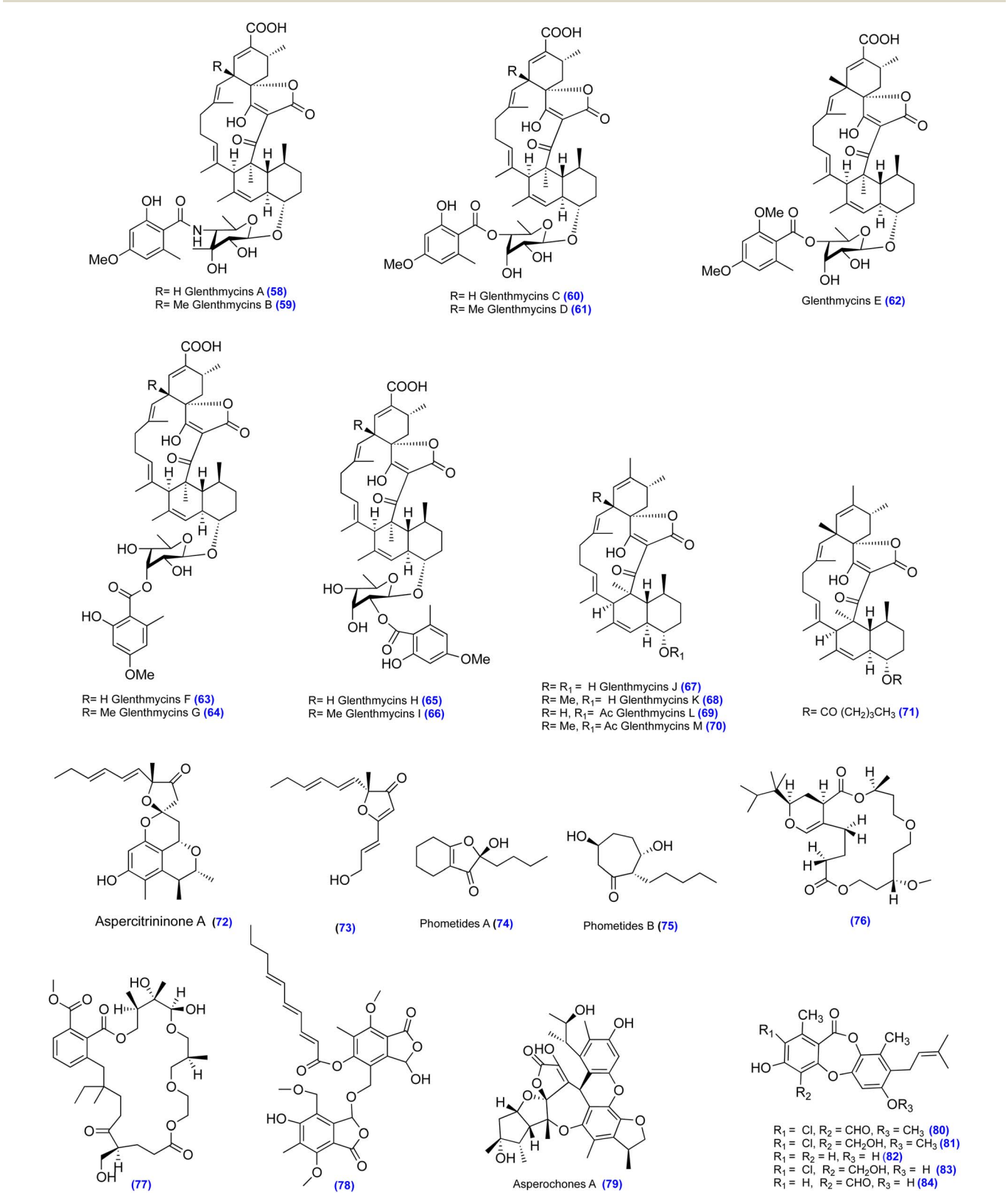

Fig. 7 Chemical structures of polyketide-based compounds (**58–84**) as antibacterial agents.

semi-synthetic derivatives inhibited Gram-positive bacteria, with IC_{50} values ranging from 0.2 to 1.6 μM. The representative compound (**71**, Fig. 7) showed better activity than the parent glenthmycins among the semi-synthetic derivatives. Compound **71** inhibited *S. aureus* ATCC 25923, *E. faecalis*, MRSA ATCC 43300, MRSA ATCC 33591, and VRE with MICs of 0.2, 0.5, 1.6, 1.4, and 1.6 μM, respectively. Most of the glenthmycins A-I, Most of the glenthmycins A-I and K-M did not show toxicity (IC_{50} > 30 μM) against human colorectal (SW620) and lung (NCI–H460) carcinoma cells.[65] In a study, the ethyl acetate extract of *Aspergillus cristatus* exhibited antibacterial activity against *S. aureus* ATCC 25923 with a MIC of 125.0 μg mL^{-1}. Furthermore, a bioassay-guided fraction of ethyl acetate extracts of *Aspergillus cristatus* led to the isolation of active compounds (**72** and **73**, Fig. 7). Notably, the compound aspercitrininone A (**72**) possessed an unprecedented tetracyclic 6/6/6/5 spiral skeleton formed by the o-quinoid form of citrinin with 2-methylterrefuranone through a Michael addition reaction. Compounds **72** and **73** demonstrated antibacterial activity against *S. aureus*,*B. subtilis*, and *E. faecalis.*[66] Yang *et al.* identified the polyketide class of compounds phometide A (**74**, Fig. 7) and phometide B (**75**, Fig. 7) from the endophytic fungus *Phoma* sp. YUD17001, which was isolated from *Gastrodia elata* Blume. Phometide A is a C_{12} polyketide having an unusual tetrahydrobenzofuran-3(2*H*)-one core with an *α*,*β*-unsaturated ketone functionality. Meanwhile, phometide B has an unprecedented structure containing a 2-pentylcycloheptan-1-one scaffold. Among them, phometide A (**74**) showed antibacterial activity against *S. aureus* and *B. subtilis.* Notably, phometide A displayed bacteriostatic activity equivalent to kanamycin. In contrast, phometide B (**75**) exhibited antifungal activity against *C. albicans* with a MIC of 16 μg mL^{-1}. Further, phometide A (**74**) and phometide B (**75**) were evaluated against five human cancer cell lines, including MCF-7, SW480, SMMC-7721, A549, and HL-60, using the MTT assay. Interestingly, the compounds phometide A and phometide B exhibited insignificant toxicity, having an IC_{50} value of >50 μM against these cell lines.[67]

Chakraborty *et al.* conducted a bioactivity-guided fractionation of the heterotrophic Gamma-proteobacterium *Shewanella algae*, which was associated with the intertidal red algae *Hypnea valentiae*. Further fractionation of the active fractions led to the isolation of the macrocyclic polyketides (**76** and **77**, Fig. 7). Compound **76** possesses dodecahydropyranotrioxacyclooctadecine-dione. In contrast, compound **77** has trioxooctadecahydro-1*H*-benzo[*o*] tetraoxacyclopentacosine-carboxylate functionalities. Compounds **76** and **77** demonstrated antibacterial activity against MRSA and VRE, with MIC between 3.1–5.0 μg mL^{-1}. The standard drugs streptomycin and chloramphenicol exhibited higher MIC against the same strains. This study confirmed that the hydrophobic descriptor of the compounds might be responsible for their antibacterial activity. Furthermore, *in silico* molecular docking studies predicted that compounds **76** and **77** bind at the allosteric sites of MRSA's penicillin-binding protein (PBP2a).[68] Wang *et al.* isolated funitatin A (**78**, Fig. 7) from the fungus *Talaromyces funiculosus* HPU-Y01, which was cultivated with the histone deacetylase inhibitor suberoylanilide hydroxamic acid. The structural feature of funitatin A represents a rare dimeric cyclopaldic acid, demonstrating potential antimicrobial activity against *Proteus species*, *E. coli*, and *Mycobacterium phlei* with MIC of 3.13, 3.13, and 6.25 μM, respectively.[69] Zhang *et al.* identified a novel fungal metabolite, asperochone A (**79**, Fig. 7), from an *Aspergillus* sp. MMC-2. Asperochone A possesses a fascinating skeleton bearing a rare 5/6/6/6/7/5/5/5 octacyclic ring system. Its oxepane ring (H) has angular fusion to form a 1,6-dioxaspiro[4.4]nonane structure, leading to the formation of a "broken" [5.5.7] trioxafenestrane. Asperochone A demonstrated broad-spectrum antibacterial activity against *S. aureus*, *B. subtilis*, and *P. aeruginosa* with MIC_{50} of 9.4, 6.4, and 2.5 μg mL^{-1}, respectively. The compound asperochone A showed moderate antimycobacterial activity against *Mycobacterium smegmatis*, inhibiting its complete growth at 80 μg mL^{-1}. In addition to antimycobacterial activity, Asperochone A (**79**) suppressed the expression of COL1A1 and ACTA2 induced by transforming growth factor β1 (TGF-β1) in LX-2 cells.[70] The fungus *Chaetomium brasiliense* possesses secondary metabolites with antibacterial properties against *S. aureus.* Keeping this in view, Zhao *et al.* carried out bioassay-guided fractionation of *Chaetomium brasiliense*. The ethyl acetate extract of *Chaetomium brasiliense* showed significant antibacterial activity against *S. aureus* and MRSA, with MIC values of 6.25 and 3.125 μg mL^{-1}, respectively. Further exploration of the active extracts led to the identification of the depsidones (polyphenolic polyketides), including mollicellin S (**80**, Fig. 7), mollicellin T (**81**, Fig. 7), mollicellin U (**82**, Fig. 7), mollicellin D (**83**, Fig. 7), and mollicellin H (**84**, Fig. 7). Among these, mollicellin S (**80**, Fig. 7) demonstrated potential activity against *S. aureus* (ATCC 6538) and MRSA (clinical isolate 309) with the same MIC of 6.25 μg mL^{-1}. The SAR study revealed that the aldehyde group at C-4 and the methoxyl group at C-7 are responsible for antibacterial activity against *S. aureus* and MRSA.[71]

Phenyltetracenoid polyketides possess a partially reduced 1-phenyltetracene core. Among these, fasamycins, formicamycins, naphthacemycins, streptovertimycins, and accramycins are produced from *Streptomyces* spp, and these compounds have antibacterial activity against Gram-positive bacteria, including MRSA and VRE. Also, these compounds exhibit antibacterial activity by acting on Poly(ADP-ribose) polymerase-1 (PARP1) and protein tyrosine phosphatase-1B (PTP-1B). Qin *et al.* reported the isolation and characterisation of formicamycins (**85–93**, Fig. 8) from *Streptomyces formicae*. They identified formicamycin A-M and fasamycin C-E metabolites, which showed antibacterial activity against MRSA and VRE. Among them, formicamycin J inhibited MRSA and VRE with MIC of 0.625 and 1.25 μM, respectively.[72]

Later, Yuan *et al.* conducted a chemical investigation of the *Streptomyces* sp. KIB-1414, a strain from the rhizospheric soil of *Polyalthia cerasoides*. A total of nineteen polyketides were isolated and evaluated for antimicrobial activities. Interestingly, all compounds showed antibacterial activities against methicillin-resistant MRSA, *S. aureus*, *B. subtilis*, and *E. coli*, with MICs ranging from 0.20 to 50.00 μg mL^{-1}. The compounds (**87**, **91**, **93**, **94**, **95**, and **100**, Fig. 8) demonstrated potential antibacterial activity against MRSA with a MIC of 1.56 μg mL^{-1}. Whereas

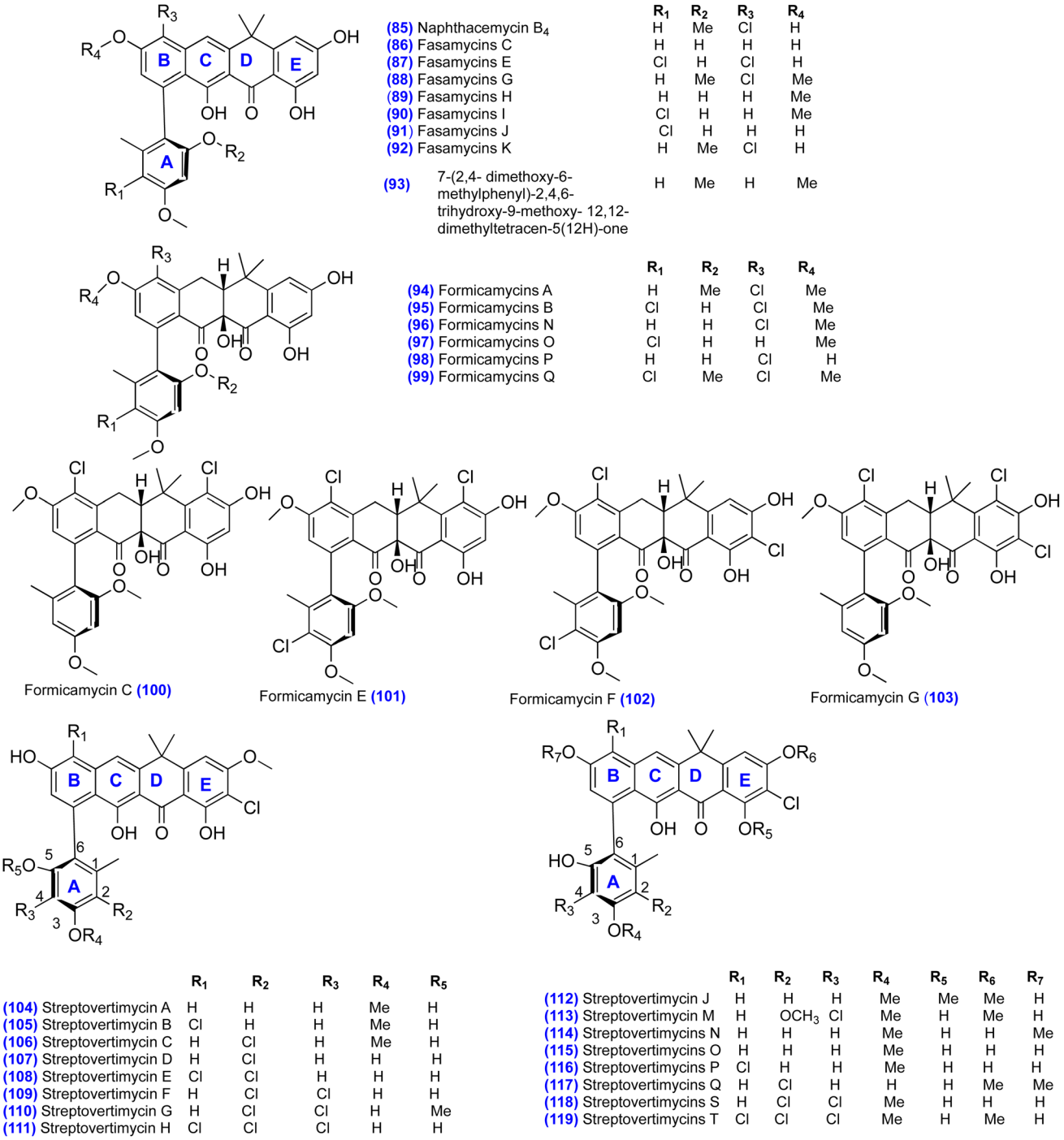

Fig. 8 Chemical structures of polyketide-based compounds (**85–119**) as antibacterial agents.

(**103**, Fig. 8) inhibited MRSA with MIC of 0.20 μg mL^{-1}, which was better than vancomycin (MIC of 1.56 μg mL^{-1}). SAR studies suggest that chlorination in the E ring is essential for antibacterial activity; the compounds (**101**, Fig. 8) demonstrated antibacterial activity against MRSA (MIC = 3.13 μg mL^{-1}) and **88** (MIC = 3.13 μg mL^{-1}), whereas the compound without chlorine substitution in **99** showed MIC of 25 μg mL^{-1}. Also, compound **103** has meta chlorine in the E ring, exhibiting the most potent antibacterial activity against *S. aureus*.[73]

In another study, Yang *et al.* identified eight fasamycin-type polyketides, streptovertimycins A-H (**104–111**, Fig. 8), from *Streptomyces morookaense* SC1169. These compounds displayed antibacterial activity against MRSA and VRE with MICs ranging between 0.63 and 5.0 μg mL^{-1}. These compounds are inactive against Gram-negative bacteria, including *E. coli* and *S. dysenteriae*. The SAR studies suggest that the free hydroxyl group at C-3 and the methoxyl group at C-5 favour antibacterial activity.

Moreover, chlorination in A and B rings disfavours the antibacterial activity.[74]

Li *et al.* worked on the *Streptomyces morookaense* SC1169 and identified several compounds, including streptovertimycins J, M, N, O, P, Q, S, and T (**112–119**, Fig. 8). These compounds (**112–119**) exhibited antibacterial activity against drug-resistant bacteria MRSA and VRE with MICs ranging from 1.25 to 10 μg mL^{-1}, respectively. In addition to antibacterial activity, these compounds **112–119** demonstrated cytotoxicity against A549, HeLa, $HepG_2$, MCF-7, and Vero cells, with IC_{50} values of 3.3, 3.9, 5.7, 5.0, and 3.0 μM, and 9.1, 7.2, 9.9, 17.8, and 14.5 μM, and 5.6, 7.0, 12.1, 24.3, and 18.9 μM, and 13.3, 15.2, 11.9, 40.3, and 33.0 μM, and 8.9, 11.0, 9.4, 21.7, and 47.0 μM, and 6.4, 5.3, 7.3, 10.7, and 13.7 μM, and 5.0, 6.0, 7.7, 14.4, and 12.4 μM, and 5.6, 9.9, 8.8, 13.9, and 12.0 μM, respectively. This finding suggests that these compounds demonstrated toxicity to human cells, which might limit the development of these compounds as antibiotics.[75]

Yang *et al.* performed a chemical analysis on the wild mushroom *Tricholoma pardinum*, which led to the isolation of the four polyketide-amino acid derivatives, pardinumones A-D (**120–123**, Fig. 9). These compounds displayed moderate antibacterial activity against *S. aureus*, *S. epidermidis*, and *E. coli*, with MIC ranging between 6.25 and 50 μg mL^{-1}.[76] Aromatic polyketides possess diverse structural compounds with significant biological properties. The bacterial-derived aromatic polyketides are usually synthesized from the type II polyketide synthase.[77] Aromatic polyketides are characterized by complex polycyclic carbon structures biosynthesized by polyketide synthases. Aromatics polyketides, such as daunorubicin and

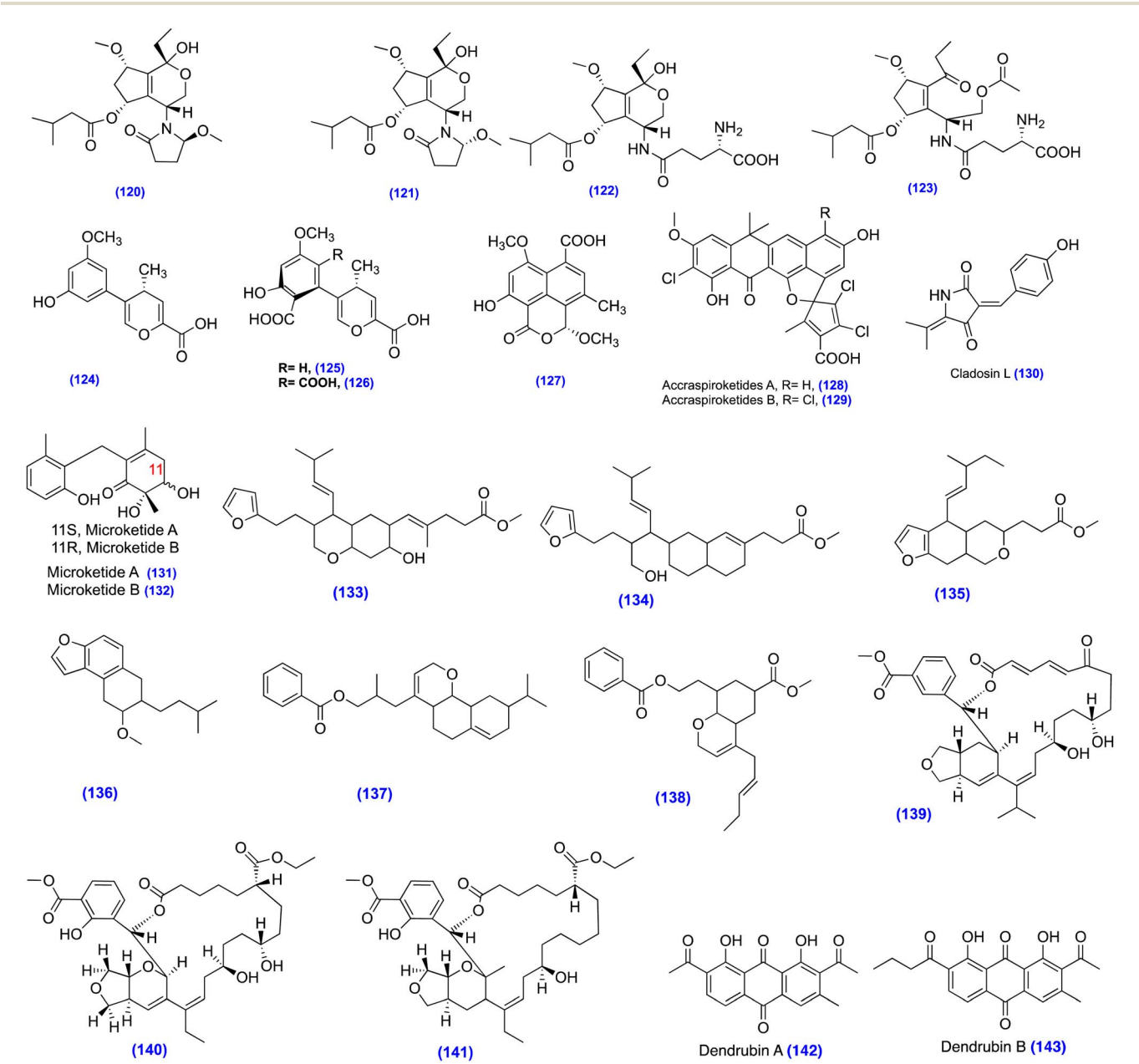

Fig. 9 Chemical structures of polyketide-based compounds (**120–143**) as antibacterial agents.

mithramycin, are well-known drugs for treating cancers. Whereas tetracycline and fasamycin C are antibiotics.[78] In a study, Orfali *et al.* conducted a chemical investigation of the *Penicillium* sp. RO-11 has reported aromatic polyketides penipyranicins A-C (**124–126**, Fig. 9) and isopyrenulin (**127**, Fig. 9). Notably, penipyranicins C (**126**) exhibited the most potent antibacterial activity against Gram-negative bacteria, especially *Enterobacter xiangfangensis* and *Pseudomonas aeruginosa.* The SAR study revealed that the presence of a carboxylic acid group is essential for antibacterial activity. Compounds, penipyranicins A and B (**124** and **125**), displayed reduced antibacterial activity due to the loss of one or two carboxylic acids in the compounds. The compound isopyrenulin (**127**) demonstrated better antibacterial activity against *Staphylococcus aureus* and *Bacillus licheniformis* and moderate activity against Gram-negative *Enterobacter xiangfangensis*.[79] Phenylnaphthacenoid polyketides have received significant attention due to their potential biological activities, including antibacterial. The soil bacteria *Streptomyces* sp. MA37 is the producer of accramycins. Maglangit *et al.* identified two polyketides, accraspiroketides A (**128**, Fig. 9) and B (**129**, Fig. 9), from the *Streptomyces* sp. MA37 Δ*accJ* mutant strain. The compounds accraspiroketides A and B possess an unprecedented [6 + 6 + 6 + 6] + [5 + 5] spiro ring system. The accraspiroketides A (**128**) and B (**129**) showed broad-spectrum antibacterial activity against *S. aureus* (ATCC 25923), *E. faecalis* (ATCC 29212), *E. faecium* K59-68, and *E. faecium* K60-39. Notably, accraspiroketides A (**128**) inhibited *E. faecium* K60-39 with a MIC of 4 μg mL^{-1}, whereas, against the same strain, ampicillin exhibited a MIC of 25 μg mL^{-1}.[80] Pan *et al.* isolated an endophytic fungus, *Cladosporium sphaerospermum* WBS017, from the healthy bulbs of *Fritillaria unibracteata* var. wabuensis. *Cladosporium sphaerospermum* fermented on solid rice medium and white bean produced different polyketides: cladosin L, M, N, O, C, B, F, cladodionen, and kahalalide F. Among these compounds, cladosin L (**130**, Fig. 9) showed moderate activity against *S. aureus* (ATCC 29213) with MIC value of 25 μM. Also, cladosin L exhibited moderate cytotoxicity against the mouse lymphoma cell line L5178Y at an initial dose of 25 μg mL^{-1}.[81]

A study by Liu *et al.* has explored the ethyl acetate fraction of the fungus *Microsphaeropsis* sp. RA10-14 led to the identification of microketide A (**131**, Fig. 9) and microketide B (**132**, Fig. 9). These compounds are C-11 epimers similar to diphenyl ketones. Microketide A and microketide B showed promising antibacterial activity against *Pseudomonas aeruginosa*,*Nocardia brasiliensis*,*Kocuria rhizophila*,*Bacillus anthracis*,*Bacillus cereus*,*Enterobacter aerogenes*,*Nocardia brasiliensis*,*Salmonella typhi*, and *Vibrio parahaemolyticus.* Moreover, the compounds also showed promising antifungal activity against *Candida albicans*,*Colletotrichum truncatum*,*Gloeosporium musarum*, and *Pestalotia calabae.*[82]

Chakraborty *et al.* explored the chemical constituents of *Bacillus subtilis* MTCC 10403, which was associated with the Brown seaweed *Anthophycus longifolius.* The bioactivity-guided fractionation of the ethyl acetate extracts of the bacteria led to the isolation of four homologous polyketide furanoterpenoids (**133–136**, Fig. 9). These polyketides demonstrated antibacterial activity against food pathogens *Vibrio parahaemolyticus*, *Aeromonas hydrophila*, *V. vulnificus*, and *V. alginolyticus*. The compounds **133** and **135** showed better antibacterial activity against food pathogens than tetracycline and ampicillin.[83] In another study, the bioactivity-guided fractionation of Heterotrophic *Bacillus amyloliquefaciens* associated with the edible red seaweed *Laurenciae papillosa* led to the isolation of the polyketide compounds (**137** and **138**, Fig. 9). These compounds inhibited food pathogens *V. parahaemolyticus* ATCC 17802™, *Vibrio vulnificus*, and *Aeromonas hydrophila.* The SAR suggests that the hydrophobic descriptor of compounds contributes to antibacterial activity.[84] Kizhakkekalam *et al.* identified oxygenated elansolid-type polyketides (**139–141**, Fig. 9) from *Bacillus amyloliquefaciens* MTCC 12716, which was found to be associated with the red alga *Hypnea valentiae.* The compound possesses an isobenzofuranyl benzoate and 1*H*-furopyrano[2,3-*c*]oxacyclononadecine-6-carboxylate moiety skeleton. Notably, these compounds exhibited better antibacterial activity than ampicillin and chloramphenicol against MRSA, VRE, *Enterococcus faecalis*, *Pseudomonas aeruginosa*, and *Klebsiella pneumoniae*. The *in-silico* study of these compounds suggests the binding of the compound to the peptide deformylase protein of *S. aureus*. Also, the compound descriptors, including higher electronic values and lipophilic parameters, support their antimicrobial activity.[85] Ishida *et al.* explored the constituents of *Dendrosporobacter quercicolus*, a member of Negativicutes, which was isolated from the discoloured heartwood of oak trees. Negativicutes are Gram-positive bacteria with an unusual cell wall that resists Gram-negative staining. They have identified dendrobiums, which are anthraquinone polyphenols. Among them, dendrobium A (**142**, Fig. 9) and dendrobium B (**143**, Fig. 9) demonstrated antibacterial activity against mycobacteria. In the assays conducted with HeLa cells, both compounds displayed no cytotoxic effects at concentrations up to 50 μg mL^{-1}. Furthermore, the antiproliferative activity of dendrobium A and B was found to be moderate against the leukemia cell line K-562. Notably, dendrobium B demonstrated a GI_{50} value of 3.6 μg mL^{-1} against HUVEC endothelial cells. This finding suggests compounds have low or minimal toxicity against human cells, and thus can be taken further for an *in vivo* model of mycobacterial infections.[86]

Vancoresmycin (**144**, Fig. 10) is a tetrameric acid-containing polyketide isolated from the actinomycete *Amycolatopsis* sp. ST 101170. It is a broad-spectrum antibiotic that acts against VRE and MRSA. Vancoresmycin demonstrates antibacterial activity by targeting the cytoplasmic membrane of Gram-positive bacteria through a non-pore mechanism. Additionally, it causes concentration-dependent depolarization in bacteria. Moreover, it shows more potent antibacterial activity against *Bacillus subtilis* than nalidixic acid and carbenicillin.[87]

Sun *et al.* conducted a chemical investigation of the mangrove sediment-associated bacteria *Streptomyces* sp. SCSIO 40069. This work identified the aromatic polyketides (**145–148**, Fig. 10), which exhibited moderate antibacterial activity against *Acinetobacter baumannii*, *S. aureus*, *K. pneumoniae*, and *M. luteus*.[88]

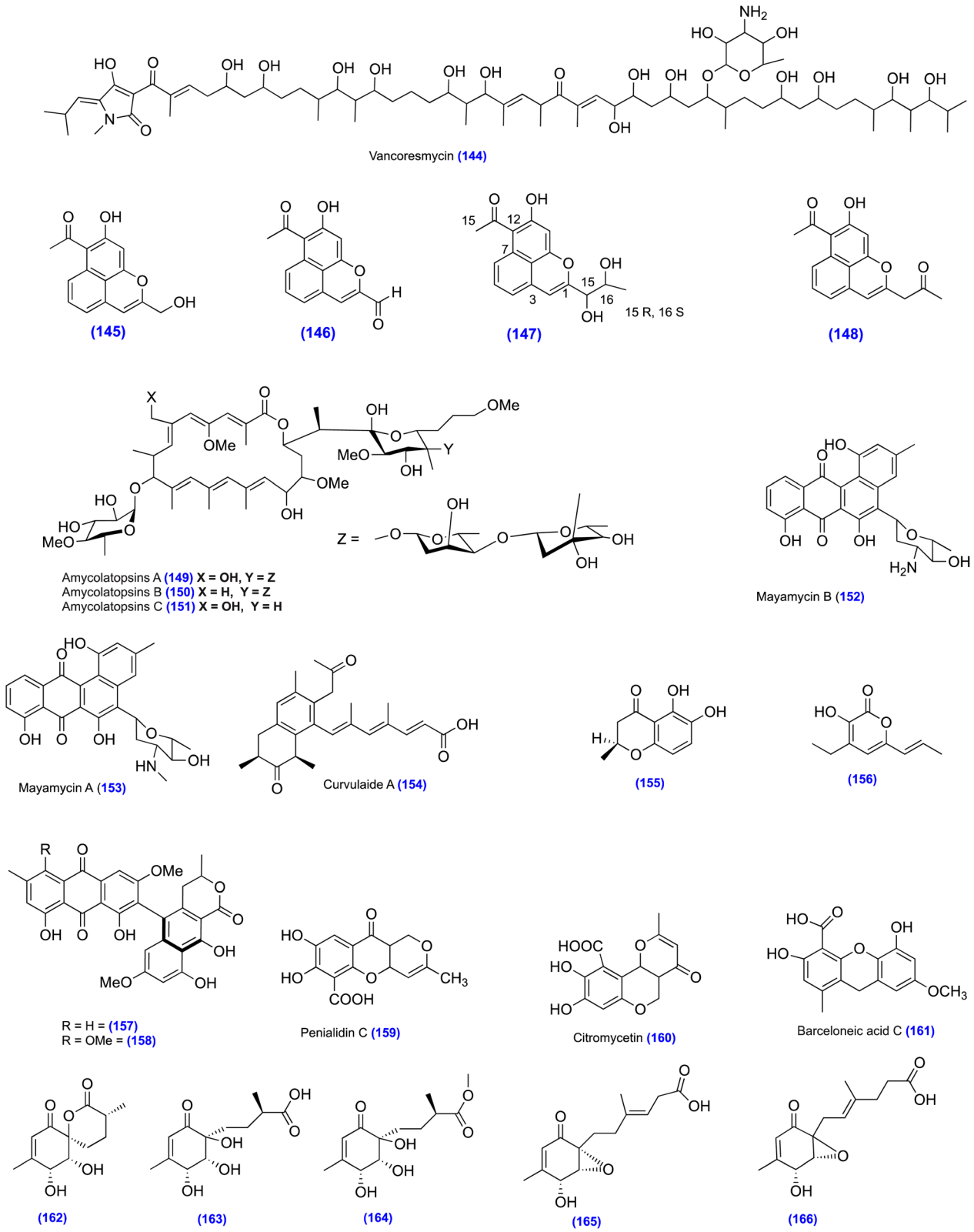

Fig. 10 Chemical structures of polyketide-based compounds (144–166) as antibacterial agents.

Khalil *et al.* explored the chemical constituents of *Amycolatopsis* sp. MST-108494. The chemical fractionation led to the identification of secondary metabolites, including glycosylated macrolactones, amycolatopsins A (**149**, Fig. 10), B (**150**, Fig. 10), and C (**151**, Fig. 10). These compounds belong to a rare class of glycosylated polyketide macrolides. Compounds **149** and **151**

showed strong inhibitory effects against *M. bovis* and *Mtb* H37Rv. The SAR studies suggest hydroxylation of the 6-methyl position is important for antimycobacterial activity. Additionally, glycoside hydrolysis enhances the antimycobacterial activity. Also, the compounds, **149–151**, were toxic to human cells and inhibited NCIH-460 and SW620 with IC_{50} values of 1.2, 0.28, and 5.9 μM, and 0.08, 0.14, and 10 μM, respectively.[89]

Bo *et al.* have identified the polyketide mayamycin B (**152**, Fig. 10), a congener of mayamycin A (**153**, Fig. 10), from *Streptomyces* sp. 120 454. The chemical structure of mayamycin features a characteristic tetracyclic benz[*a*] anthracene scaffold. Mayamycin A and mayamycin B exhibited potent antibacterial activity against *Micrococcus luteus*. Additionally, these polyketides displayed moderate antibacterial activity against *S. aureus*,*S. pyogenes*,*B. subtilis*, and *P. aeruginosa*.[90]

The *Curvularia* sp. IFB-Z10 was initially isolated from the gut flora of the fish *Argyrosomus argentatus*. It is known to produce alkaloids, including curvulamine and curindolizine. Liu *et al.* cultured *Curvularia* sp. IFB-Z10, through solid-state fermentation using rice as a substrate, led to the isolation of a new bicyclic polyketide curvulaide A (**154**, Fig. 10). Notably, curvulaide A showed moderate antibacterial activity against the anaerobic bacteria *Porphyromonas gingivalis* with a MIC of 62.5 μM. However, this compound showed moderate cytotoxicity against cancer cells, human hepatoma cell lines BEL7402, BEL7402/5-Fu with IC_{50} values of 19.85 and 12.46 μM, which might limit its scope for developing as an antibiotic.[91] *Colletotrichum gloeosporioides* is a plant fungal pathogen. It is reported to produce metabolites such as aspergillomarasmine A and B, and colletotric acid. In a study, Luo *et al.* cultured the fungus *Colletotrichum gloeosporioides* and explored the metabolites produced from it, leading to the isolation of polyketides including (2*S*)-2,3-dihydro-5,6-dihydroxy-2-methyl-4*H*-1-benzopyran-4-one (**155**, Fig. 10) and 4-ethyl-3-hydroxy-6-propenyl-2*H*-pyran-2-one (**156**, Fig. 10). These compounds showed moderate antibacterial activity against *Bacillus subtilis* and *S. aureus*.[92]

Boudesocque-Delaye *et al.* conducted a phytochemical investigation of the tubers of *Pyrenacantha kaurabassana*, resulting in the isolation of heterodimer polyketides (**157** and **158**, Fig. 10) that exhibited antagonist activity against *S. aureus* and *H. pylori*.[93]

Jouda *et al.*, while working with the liquid culture obtained from the fermentation of *Penicillium* sp., isolated polyketide-based compounds penialidins A-C, citromycetin, p-hydroxy phenyl glyoxalaldoxime, and Brefeldin A. Penialidins C (**159**, Fig. 10) and citromycetin (**160**, Fig. 10) exhibited moderate antibacterial activity against *M. smegmatis*.[94]

Xia *et al.* isolated the endophytic fungus *Phoma* sp. JS752 from the plant *Phragmites communis* Trinus. Furthermore, culturing the fungus *Phoma* sp., followed by extraction with organic solvents and chromatographic separation, led to the identification of the polyketides barceloneic acid C, barceloneic acid A, and questin. Previous research suggested that barceloneic acids A, B, and barceloneic lactone are reported to inhibit farnesyl protein transferase. Among the isolated compounds, barceloneic acid C (**161**, Fig. 10) exhibited potent antibacterial activity against the Gram-positive bacteria *L. monocytogenes* and *S. pseudintermedius*, with showing MIC of 1.02 μg mL^{-1}. Meanwhile, ampicillin demonstrated antibacterial activity against both strains with MIC value of 0.89 μg mL^{-1}.[95]

Guo *et al.* cultured and activated the silent genes of the fungus *Penicillium* sp. F23-2, using OSMAC to produce secondary metabolites. The fungus was cultured on rice solid medium, and further chromatography and NMR spectral analysis led to the identification of polyketide-based ambuic acid analogues, penicyclones A-E (**162–166**, Fig. 10). Interestingly, all compounds showed potent antibacterial activity against *S. aureus*, with MICs ranging between 0.3 and 1 μg mL^{-1}. These compounds share common structural features of highly functionalised cyclohexanones with a carboxylic acid in their side chain.[96]

4. Polyketides-based leads as antimalarial agents

Malaria is a disease caused by a protozoan parasite, primarily transmitted by infected Anopheles mosquitoes. It affects millions annually, leading to significant illness and mortality, especially in vulnerable populations in tropical and subtropical regions.[97] Despite extensive research and interventions, malaria remains a major global health challenge.[98] *Plasmodium* spp., including *Plasmodium falciparum*, *Plasmodium vivax*, *Plasmodium ovale*, and *Plasmodium malariae*, are the parasites responsible for causing malaria in humans. *P. falciparum* is a notorious parasite that accounts for about 99% of malaria deaths worldwide.[99] *Plasmodium knowlesi*, a type of monkey malaria, has been identified as the fifth malarial parasite affecting humans and is primarily reported in Southeast Asia.[100]

Chianese *et al.* conducted a chemical investigation of the sponge *Plakortis simplex*, leading to the isolation of several endoperoxides. Among these, the representative compounds plakortin (**167**, Fig. 11) and dihydroplakortin (**168**, Fig. 11) demonstrated antimalarial activity against D10 (chloroquine-sensitive), W2 (chloroquine-resistant), and *P. falciparum*.[101] Moreover, plakortin (**167**) exhibits antiparasitic activity against *P. falciparum* with an IC_{50} of $\leq$ 1 μM. Plakortin induces dose- and time-dependent morphological anomalies, early maturation delays, reactive oxygen species (ROS) generation, and lipid peroxidation in the parasite. Additionally, it results in significant lipid peroxidation and a four-fold increase in the lipoperoxide breakdown product, 4-hydroxynonenal. Notably, the 4-hydroxynonenal displayed binding to several essential proteins of *P. falciparum*.[102]

Shi *et al.* explored the mesophilic fungus *Geomyces auratus*,*which belongs* to the Myxotriachaceae family, for its chemical constituents. This research led to the identification of georatusin (**169**, Fig. 11), which possesses a unique structural feature characterized as a hybrid of polyketides and peptides. Georatusin showed antiparasitic activity against *Leishmania donovani* and *Plasmodium falciparum.* Moreover, georatusin did not show any toxicity (>100 μM) to the mammalian L6 cells, and can be taken for further in-depth biological study.[103]

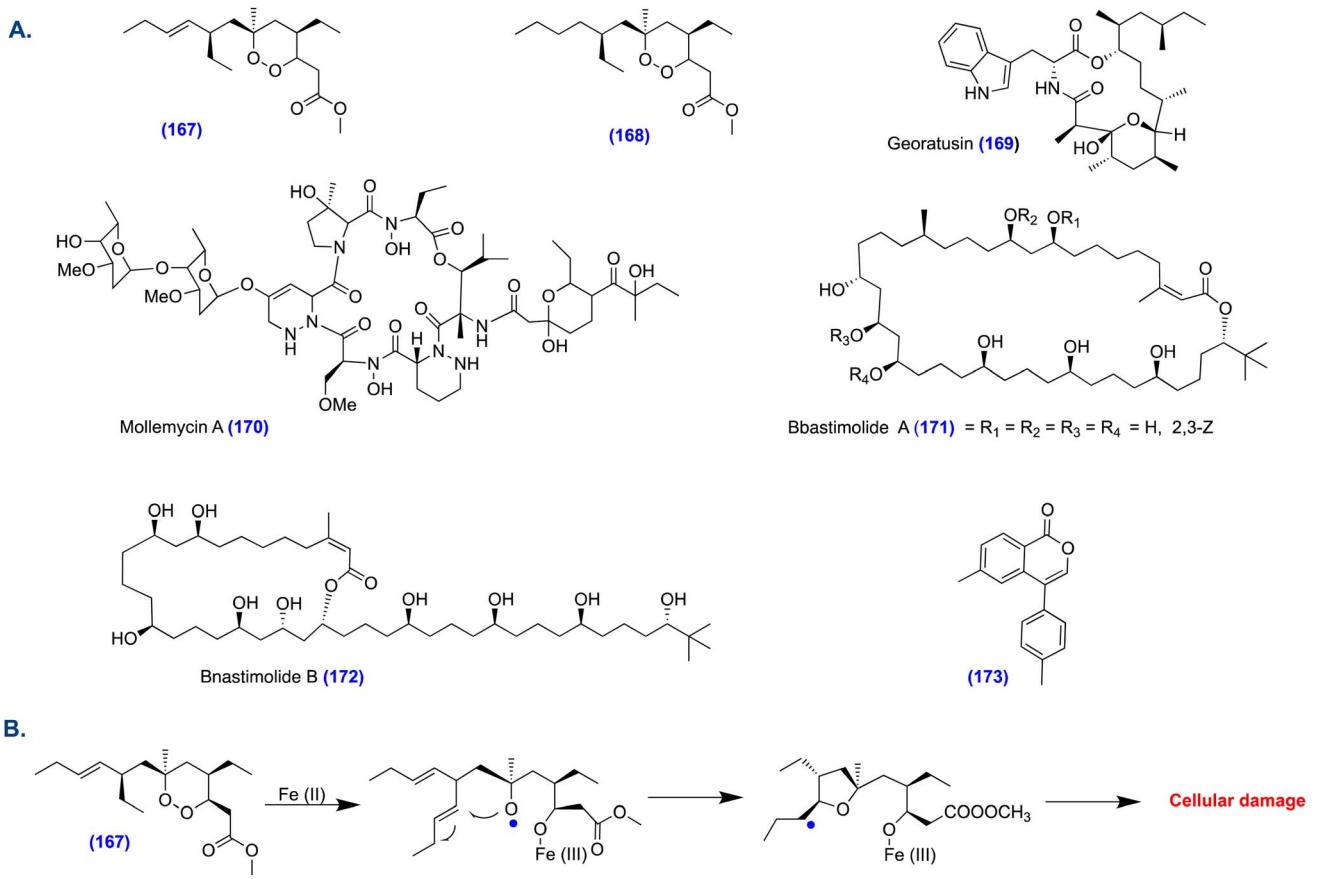

Fig. 11 (A) Polyketides-based compounds (**167–173**) as antimalaria. (B) Chemical representation depicting plakortin as reactive oxygen generation and lipid peroxidation.

Raju *et al.* explored the secondary metabolites present in the antibacterial extract of a *Streptomyces* sp. (CMB-M0244), leading to the identification of compound mollemycin A (**170**, Fig. 11), which displayed exceptionally potent antibacterial activity against Gram-positive and Gram-negative bacteria, *Mycobacterium bovis*, and antimalarial activity against *P. falciparum*. However, it showed moderate toxicity to human neonatal foreskin fibroblast cells with an IC_{50} value of 198 nM, which might limit the development of the compound as a therapeutic candidate.[104]

Shao *et al.* isolated polyketide-based macrolides bastimolide A (**171**, Fig. 11) and bastimolide B (**172**, Fig. 11) from the tropical marine cyanobacterium *Okeania hirsute*. Bastimolide A is a cyclic macrolide, whereas bastimolide B is a 24-membered polyhydroxymacrolide featuring a long aliphatic chain and a unique terminal *tert*-butyl group. Both bastimolide A and bastimolide B demonstrated potent antimalarial activity against *P. falciparum*. Each natural compound possesses unique terminal *tert*-butyl groups.[105]

Amorim *et al.* conducted bioassay-guided fractionation of the ethyl acetate soluble extract from a culture of the marine-derived fungus *Peroneutypa* sp. M16 strain, leading to the identification of several polyketide terpenoid metabolites. Among these, metabolite (**173**, Fig. 11) exhibited moderate antimalarial activity against *P. falciparum* chloroquine-sensitive and resistant strains.[106]

5. Polyketides-based leads as antifungal

The annual incidence of fungal infections is significantly high for chronic pulmonary aspergillosis, cryptococcal meningitis, invasive candidiasis, and *Pneumocystis jirovecii* pneumonia.[107] Fungal infections predominantly start on the skin and are generally superficial. However, if these infections progress, they can enter the systemic circulation. There are two primary types of fungal infections: superficial mycoses and systemic mycoses. Superficial mycoses remain limited to the outer layers of the skin, whereas systemic mycoses can affect the body's internal organs.[8] The treatment of mycoses is effectively managed with five primary classes of antimycotic drugs: azoles, polyenes, echinocandins, allylamine, and antimetabolites (Fig. 12). Each of these classes operates through distinct mechanisms to successfully combat fungal infections.[108] In recent decades, fungal pathogens have developed antibiotic resistance, leading to treatment failures and severely compromising clinical outcomes for patients with life-threatening fungal infections. This resistance limits available treatment options and

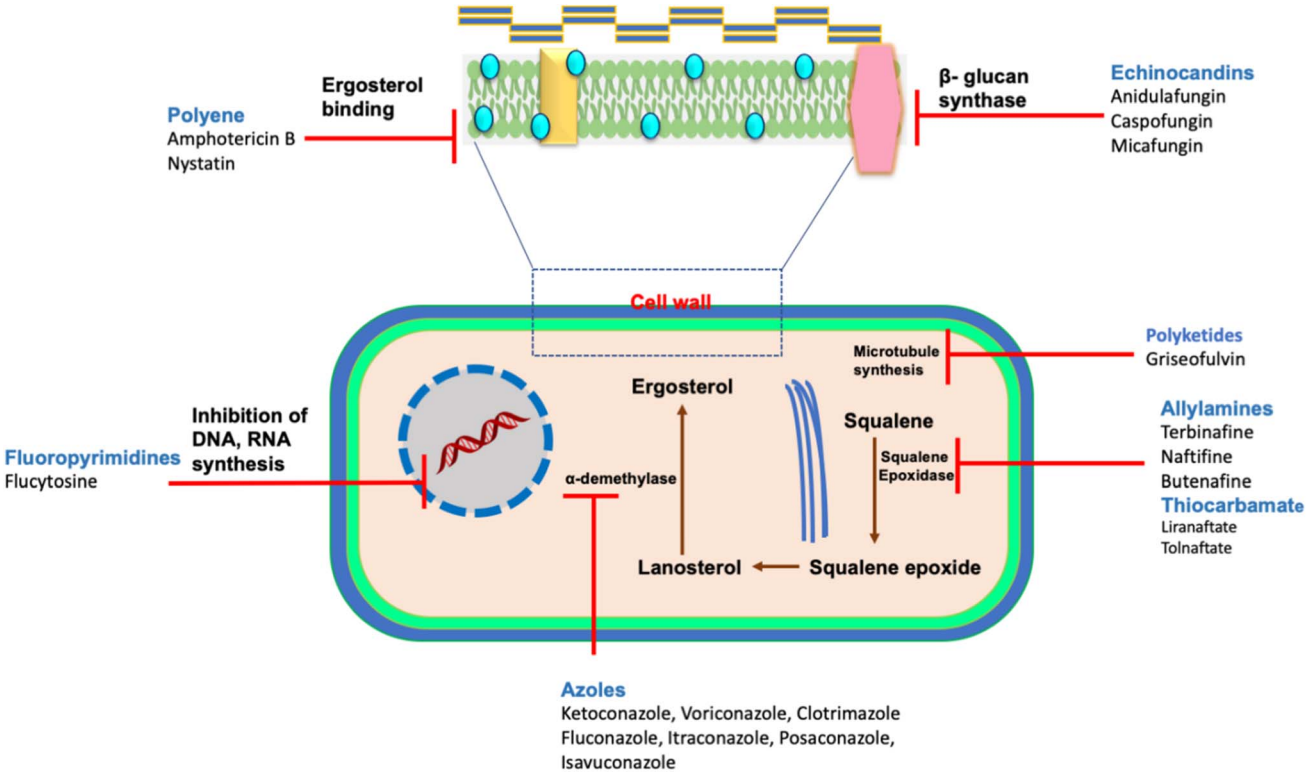

Fig. 12 A pictorial representation depicting a fungal cell with its targets and inhibitors.

highlights the need for new agents with novel mechanisms of action to combat these infections effectively.[109,110]

Wang *et al.* have identified canecines A-B (**174** and **175**, Fig. 13) from an extract of the fungus *Penicillium canescens* DJJ-1 associated with *Aconitum brevicalcaratum.* Notably, the compound canecines A displayed significant activity against *C. albicans*, with a MIC value of 1 μg mL^{-1}, whereas the standard drug nystatin had a MIC value of 2 μg mL^{-1}. Canecines A (**174**) and canecines B (**175**) exhibited moderate antibacterial activity against *B. subtilis* and *E. coli*, with MIC values of 64, 64, and 32, 64 μg mL^{-1}, respectively. The antibacterial activity was less than that of the standard drug kanamycin.[111]

Weider *et al.* conducted bioassay-guided isolation of the fungus *Acrophialophora levis to* identify antifungal compounds, resulting in the isolation of the polyhydroxy-polyketides acrophialocinol (**176**, Fig. 13) and acrophialocin (**177**, Fig. 13). Both acrophialocinol and acrophialocin exhibited broad-spectrum antifungal activity against *M. oryzae*, *B. cinerea*, *F. graminearum*,*A. oryzae*,*P. infestans*, and *C. albicans.*[112]

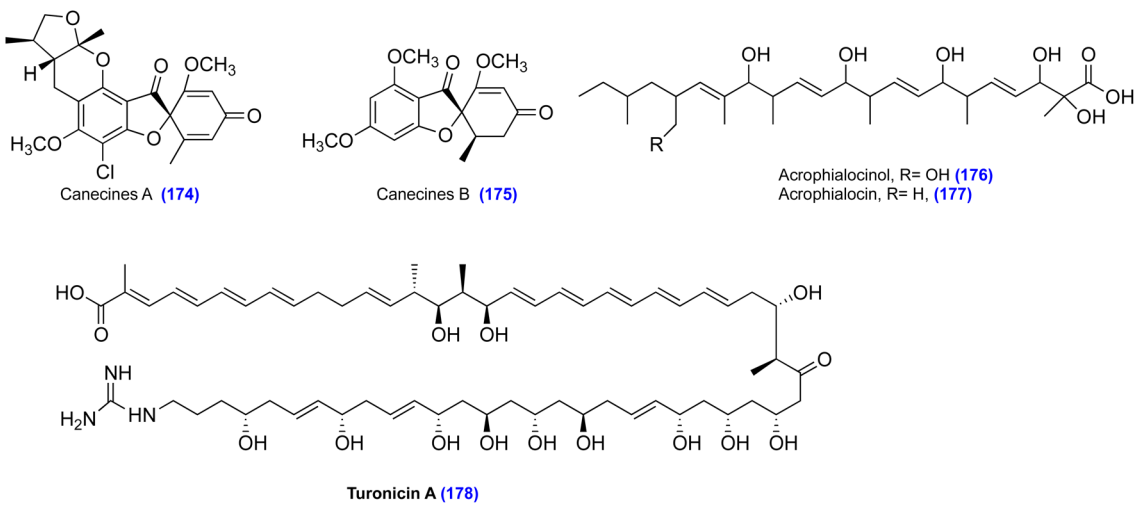

Fig. 13 Polyketide-based compounds (**174–178**) as antifungal agents.

Table 2 Potent polyketide-based antimicrobial leads

Microorganism	Compound name		Mode of action	Targeted	Ref.
Bacteria	**23**	*Bacillus amyloliquefaciens* MTCC 12713		Compound **23** inhibited bacteria, including *E. coli*, *V. parahaemolyticus*,*P. aeruginosa*,*K. pneumoniae*,*E. tarda*,*S. pyogenes*, MRSA, VRE*fs* with MIC values of 3.12, 1.56, 1.56, 1.56, 3.12, 1.56, 1.56. and 1.56 μg mL^{-1}, respectively	44
Bacteria	O^4–Me-tetracenomycin C (**34**)	*Amycolatopsis* sp. strain A23		Compound **34** inhibits *E. coli* with a MIC value of 16 μg mL^{-1}	47
Fungi	Erythromycin TMC-154 (**35**)	*Clonostachys rogersoniana*	Erythromycin TMC-154 acts by stimulating the formation of ROS in *S. pyogenes*	TMC-154 inhibits *S. aureus*, *S. pyogenes*, *S. mutans*, *P. aeruginosa*, and *V. parahaemolyticus* with MIC values of 125, 25, 25, 62.5, and 62.5 μM, respectively	48
Bacteria	Kalimantacin A (**36**)	*Pseudomonas fluorescens*	Kalimantacin A acts by inhibiting the FabI of *S. aureus*	Kalimantacin A inhibits *S. aureus* ATCC6538 and *S. aureus* RN4220 with MIC value of 0.125 μg mL^{-1}	49 and[50]
Bacteria	Cervimycins C (**38**)	*Streptomyces tendae* HKI 0179	It acts on the membrane of the *B. subtilis* 168 and *S. aureus.* Moreover, in low concentrations, it acts on DNA gyrase	Cervimycins C inhibits *B. subtilis* 168 and *S. aureus* SG511 Berlin, with MIC values of 0.25 and 2 mg L^{-1}	51
Bacteria	Stictamycin (**39**)	*Streptomyces* sp. 438-3		Stictamycin inhibits *B. subtilis* E168, *E. coli* (TolC-deficient), and *S. aureus* with MIC values of 32, 32, and 2 μg mL^{-1}, respectively	52
Bacteria	Gladiolin (**40**)	*Burkholderia gladioli*	It acts on the bacterial RNA polymerase	It acts on the *Neisseria gonorrhoeae* with MIC values ranging between 1–2 mg mL^{-1}	56
Bacteria	Argenteolides A (**41**) and B (**42**)	*Streptomyces argenteus*		Argenteolides A and B inhibited *Staphylococcus aureus* and *Escherichia coli* ATCC25922 with MIC values of 11.6, 21.0 μg mL^{-1} and 15.7, 27.9 μg mL^{-1}, respectively	58
Bacteria	Difficidin analogues (**44–47**)	*Bacillus amyloliquefaciens* MTCC12713		**44** inhibited MRSA, VRE*fs P. aeruginosa*,*K. pneumonia*,*E. tarda*,*E. coli*, *S. pyogenes*, and *V. parahaemolyticus* with zone of inhibition (ZOI) values of 21, 22, 17, 19, 22, 19, 21, and 25 mm, and **45** showed ZOI values of 30, 32, 26, 30, 26, 27, 26, and 24 mm and **46** showed ZOI values of 26, 24, 23, 29, 26, 24, 20, and 23 mm and **47** showed ZOI values of 25, 24, 25, 31, 27, 29, 30, and 33 mm, respectively	60
Bacteria	Bacillibactin analogues (**48–51**)	*Bacillus amyloliquefaciens* MTCC12713		**48** inhibited *E. coli*, *V. parahaemolyticus*, *P. aeruginosa*, *K. pneumonia*, *E. tarda*, *S. pyogenes*, MRSA, VRE*fs*, with ZOI values of 18, 20, 17, 10, 20, 23, 21, and 23 mm, and **49** showed ZOI values of 20, 27, 15, 15, 26, 22, 23, 24 mm and **50** showed ZOI values of 30, 32, 24, 26, 28, 29, 25, and 29 mm, and **51** showed ZOI values of 23, 27, 21, 22, 27, 20, 22, and 25 mm, respectively	61

Table 2 (*Contd.*)

Microorganism	Compound name		Mode of action	Targeted	Ref.
Fungus	Xanthoepocin (**52**)	*Penicillium ochrochloron*		Xanthoepocin inhibited *S. aureus* with a MIC value of 0.313 μg mL^{-1}. It also inhibited LVRE with the MIC value ranging from 0.078–0.313 μg mL^{-1}	62
Bacteria	Wychimicins A-D (**53–56**)	*Actinocrispum wychmicini*		**53, 54, 55,** and **56** inhibited *S. aureus* FDA209P with MIC values of 0.125, 0.25, 0.125, and 0.5 μg mL^{-1} **53, 54, 55,** and **56** inhibited *Bacillus cereus* ATCC10702 with MIC values of 0.25, 0.5, 0.5, and 2 μg mL^{-1} **53, 54, 55,** and **56** inhibited *Corynebacterium bovis* 1810 with MIC values of 0.25, 0.5, 0.5, and 2 μg mL^{-1} **53, 54, 55,** and **56** inhibited *Enterococcus faecalis* JCM5803 with MIC values of 0.25, 0.5, 0.25, and 1 μg mL^{-1} **53, 54, 55,** and **56** inhibited *Enterococcus faecium* JCM5804 with MIC values of 0.25, 0.5, 0.25, and 1 μg mL^{-1}	63
Bacteria	(−)-Tatiomicin (**57**)	*Amycolatopsis* sp. DEM30355	It causes membrane depolarisation and chromosome decondensation in the bacteria	(−)-Tatiomicin displayed antibacterial activity against *Staphylococcus* and *Streptococcus* species, with the MIC ranging between 4–8 μg mL^{-1}	64
Bacteria	Glenthmycins A-I (**58–66**) glenthmycins K-M (**68–71**)	*Streptomyces* sp. CMB-PB041		Glenthmycins A-I and K-M inhibited *S. aureus* with MIC values of 6.4, 11.9, 15.3, >30, 4.9, 8.4, 23.2, 18.4, 10.0, and 16.4, 0.8, 1.2 μM, respectively Glenthmycins A-I and K-M inhibited *E. faecalis* with the MIC values of 5.7, 7.3, 3.1, >30, 6.2, 8.9, 4.0, 2.7, 13.0, and >30, 3.0, 3.7 μM, respectively Glenthmycins A-I and K-M inhibited MRSA ATCC 43300 with the MIC values of 4.4, 9.1, 6.3, >30, 3.9, 7.9, 7.3, 16.3, 15.2, and 3.8, 0.3, 1.1 μM, respectively Glenthmycins A-I and K-M inhibited VRE with the MIC values of 5.2, 9.5, 5.4, >30, 3.2, 2.9, 13.1, 2.9, 7.3, and >30, 6.7, 10 μM, respectively	65
Fungus	Aspercitrininone A (**72**) and (**73**)	*Aspergillus cristatus*		**72** inhibited *S. aureus* ATCC 25923, *B. subtilis* ATCC 6633, and *E. faecalis* ATCC 29212 with MIC values of 26.3, 22.5, and 67.3 μg mL^{-1}, respectively, and **73** inhibited *S. aureus* ATCC 25923, *B. subtilis* ATCC 6633, and *E. faecalis* ATCC 29212 with MIC values of 18.6, 13.2, and 45.9 μg mL^{-1}, respectively	66

Table 2 (*Contd.*)

Microorganism	Compound name	Mode of action	Targeted	Ref.
Fungus	Phometide A (**74**) and phometide B (**75**)	Fungus *Phoma* sp. YUD17001	Phometide A (**74**) shows antibacterial activity against *Staphylococcus aureus* with MIC values of 4 μg mL^{-1}. **75** exhibited antifungal activity against *C albicans* with a MIC value of 16 μg mL^{-1}	67
Algae	(**76** and 77)	*Gamma-proteobacterium Shewanella*	**76** inhibited MRSA ATCC 33592, VREfs ATCC 51299, and *E. coli* MTCC 443 with MIC values of 5.0, 3.12, and 3.12 μg mL^{-1}, whereas 77 inhibited the same strains, with MIC values of 3.12, 3.0, and 3.12 μg mL^{-1}, respectively	68
Fungus	Funitatin A (**78**)	*Talaromyces funiculosus*	**78** exhibited antibacterial activity against *Proteus species*, *E. coli*, and *Mycobacterium phlei* with MIC values of 3.13, 3.13, and 6.25 μM, respectively	69
Fungus	Asperochone A (**79**)	*Aspergillus* sp. MMC-2	Asperochone A (**79**) showed activity against *S. aureus*, *B. subtilis*, and *P. aeruginosa* with MIC_{50} values of 9.4, 6.4, and 2.5 μg mL^{-1}, respectively	70
Fungus	Mollicellin S–U (**80–84**)	*Chaetomium brasiliense*	**80–84** inhibited *S. aureus* (ATCC 6538) and MRSA (clinical isolate 309) with MIC values of 6.25, 6.25, 12.5, and 12.5, 12.5, and 25, >100, and >100 and 25, and 25 μg mL^{-1}, respectively	71
Bacteria	Formicamycin G (**103**)	*Streptomyces* sp. KIB-1414	**103** inhibited MRSA with a MIC value of 0.20 μg mL^{-1}	73
Bacteria	Streptovertimycin G (**110**)	*Streptomyces morookaense* SC1169	Streptovertimycin G showed potent antibacterial activity against MRSA, MSSA, VRE, and VSE with the same MIC values of 0.63, 0.63, 1.25, and 1.25 μg mL^{-1}	74
Bacteria	Streptovertimycin M (**113**)	*Streptomyces morookaense* SC1169	Streptovertimycin M inhibited MRSA, MSSA, VRE, and VSE with MIC values of 1.25, 1.25, 5.0, and 2.5 μg mL^{-1}	75
Fungus	Pardinumones D (**123**)	*Tricholoma pardinum*	Pardinumones D inhibited *S. aureus*, *S. epidermidis*, and *E. coli*, with MIC values of 6.25, 6.25, and 12.5 μg mL^{-1}, respectively	76
Fungus	Penipyranicins C (**126**)	*Penicillium* sp. RO-11	Penipyranicins C inhibited *Enterobacter xiangfangensis* and *Pseudomonas aeruginosa*, with MIC values of 0.9 and 1.4 μg mL^{-1}, respectively. Isopyrenulin inhibited *Bacillus licheniformis* with a MIC value of 3.8 μg mL^{-1}	79
Bacteria	Accraspiroketides A (**128**) and B (**129**)	*Streptomyces* sp. MA37 Δ*accJ*	Accraspiroketides A inhibited *S. aureus* (ATCC 25923), *E. faecalis* (ATCC 29212), *E. faecium* K59-68, and *E. faecium* K60−39 with MIC values of 3.1, 3.1, 1.5, and 4.0 μg mL^{-1}, and against these strains, accraspiroketides B with MIC values of 6.3, 3.1, 1.5, and 4.7 μg mL^{-1}, respectively	80

Table 2 (*Contd.*)

Microorganism	Compound name	Mode of action	Targeted	Ref.
Fungus	Cladosin L (**130**)	*Cladosporium sphaerospermum* WBS017	Cladosin L inhibited *S. aureus* (ATCC 29213) and *S. aureus* (ATCC 700699) with MIC values of 50 and 25 μM, respectively	81
Fungus	Microketide A (**131**) and microketide B (**132**)	*Microsphaeropsis* sp. RA10-14	Microketide A inhibited *Bacillus subtilis*, *Bacillus anthracis*, *Bacillus cereus*, *Bacillus megaterium*, *Enterobacter aerogenes*, *Escherichia coli*, *Kocuria rhizophila*, *Micrococcus lysodeikticus*, *Nocardia brasiliensis*, *Proteus vulgaris*, *Pseudomonas aeruginosa*, *Salmonella typhi*, *Salmonella paratyphi B*, *Shigella dysenteriae*,*Vibrio parahaemolyticus*, *Candida albicans*, *Colletotrichum truncatum*, *Gloeosporium musarum*, and *Pestalotia calabae* with the MIC values of 0.19, 0.19, 0.19, 0.19, 0.19, 1.56, 0.19, 0.39, 0.19, 0.39, 0.19, 0.19, 0.19, 3.13, 0.39, 1.56, 1.56, 3.13, and 1.56 μg mL^{-1}, and microketide B inhibited the same strains with the 1.56, 0.39, 0.39, 0.19, 1.56, 3.13, 0.39, 0.78, 0.39, 1.56, 1.56, 0.19, 0.39, 6.25, 3.13, 3.13, 3.13, 3.13, and 3.13 μg mL^{-1}, respectively	82
Bacteria	Polyketide furanoterpenoids (**133**)	*Bacillus subtilis* MTCC 10403	**133** inhibited *V. parahaemolyticus ATCC® 17802™*, *A. hydrophila MTCC 646*, *V. vulnificus MTCC 1145*, *V. alginolyticus* MTCC 4439, *and V. parahaemolyticus MTCC 451* with the MIC values of 6.25, 3.12, 3.12, 6.25, and 3.12 μg mL^{-1}, respectively	83
Bacteria	Chromene polyketide (**137**, **138**)	*Bacillus amyloliquefaciens*	**137** and **138** inhibited *V. parahaemolyticus* ATCC 17802 ™ and *Aeromonas hydrophila* with ZOI values of 14, 16 mm, and 12, 14.3 mm, respectively	84
Bacteria	Oxygenated elansolid-polyketides (**139–141**)	*Bacillus amyloliquefaciens* MTCC 12716	**139** inhibited MRSA, VREfs, *Pseudomonas aeruginosa*, *Klebsiella pneumoniae*, *Edwardsiella tarda Escherichia coli*, *Streptococcus pyogenes*, *Vibrio parahaemolyticus* with MIC values of 3.00, 3.00, 3.12, 3.00, 3.12, 5.00, 5.00, and **125** inhibited the same strains with MIC values of 3.12 μg mL^{-1}, and 0.38, 1.50, 0.75, 1.50, 3.12, 0.75, 1.50, and 0.38 μg mL^{-1}, and **126** inhibited the same strains with MIC values of 1.50, 3.12, 1.50, 1.50, 3.00, 1.50, 3.12, and 1.50 μg mL^{-1}, respectively	85

Table 2 (*Contd.*)

Microorganism	Compound name	Mode of action	Targeted	Ref.
Bacteria	Dendrobium A (**142**) and dendrobium B (**143**)	*Dendrosporobacter quercicolus*	Dendrobium A inhibited *Mycobacterium vaccae* DSM43514, *Mycobacterium fortuitum* Borstel, *Mycobacterium marinum* GB 9095-0088, *Mycobacterium tuberculosis* H37Rv, and *Mycobacterium kansasii* GB 9134-0011 with MIC values of 1.56, 12.5, 5.24, 3.13, and 12.5, μg mL^{-1}, respectively. In contrast, dendrobium B inhibited *Mycobacterium vaccae* DSM43514, *Mycobacterium fortuitum* Borstel, *Mycobacterium marinum* GB 9095-0088, *Mycobacterium tuberculosis* H37Rv, and *Mycobacterium kansasii* GB 9134-0011 with MIC values of 1.56, 6.25, 0.78, 0.78, and 1.56, μg mL^{-1}, respectively	86
Bacteria	Vancoresmycin (**144**)	*Amycolatopsis* sp. ST 101170	It inhibits L-form of *Bacillus subtilis* with a MIC value of 0.0025 μg mL^{-1}	87
Bacteria	Aromatic polyketides (**145–148**)	*Streptomyces* sp. SCSIO 40069	**145, 146, 147,** and **148** inhibited *A. baumannii*, *S. aureus* ATCC 29213, *K. pneumoniae* ATCC 13883, and *M. luteus* SCSIO ML01 with MIC values of 64, 8, 64, and 8 μg mL^{-1}, and >64, >64, 32, and 32 μg mL^{-1}, and 32, >64, 16, and 64 μg mL^{-1}, and >64, 8, 8, and 8 μg mL^{-1}, respectively	88
Bacteria	Amycolatopsin A (**149**), amycolatopsins C (**151**)	*Amycolatopsis* sp. MST-108494	**149** and **151** inhibited *M. bovis* and *M. tb* H37Rv with MIC values of 0.4 and 4.4 μg mL^{-1} and 2.7 and 5.7 μg mL^{-1}, respectively	89
Bacteria	Mayamycin B (**152**) mayamycin A (**153**)	*Streptomyces* sp. 120 454	**152** and **153** inhibited *M. luteus* with MIC values of 2.0 and 8.0 μM, respectively	90
Fungus	Curvulaide A (**154**)	*Curvularia* sp. IFB-Z10	Curvulaide A (**154**) inhibited *Porphyromonas gingivalis* with a MIC value of 62.5 μM	91
Fungus	(**155**), and (**156**)	*Colletotrichum gloeosporioides*	**155** inhibited *Bacillus cereus*, with a MIC value of 12.5 μg mL^{-1}, and **156** inhibited *B. subtilis*, *S. aureus*, *and S. albus*, with the same MIC value of 12.5 μg mL^{-1}, respectively	92
Plant	Heterodimers polyketides (**157** and **158**)	*Pyrenacantha kaurabassana*	**157** and **158** inhibited *Helicobacter pylori* with the MIC value of 0.42 and 6 μM, respectively	93
Fungus	Penialidins C (**159**), and citromycetin (**160**)	*Penicillium* sp	Penialidins C (**159**) and citromycetin (**160**) inhibited *Mycobacterium smegmatis* with MIC values of 15.6 and 31.2 μg mL^{-1}, respectively	94
Fungus	Barcelone acid C (**161**)	*Phoma* sp. JS752	Barcelone acid C (**161**) inhibited *L. monocytogenes* and *S. pseudintermedius*, with the same MIC value of 1.02 μg mL^{-1}	95
Fungus	Penicyclones A–E (**162–166**)	*Penicillium* sp. F23-2	Penicyclones A-E (**162–166**) inhibited *S. aureus*, with MIC values of 0.3, 1.0, 0.9, 0.8, and 0.5 μg mL^{-1}, respectively	96

Table 2 (*Contd.*)

Microorganism	Compound name	Mode of action	Targeted	Ref.
Sponge	Plakortin (**167**) and dihydroplakortin (**168**)	*Plakortis simplex*	Plakortin (**167**) and dihydroplakortin (**168**) inhibited D10 (chloroquine sensitive) and W2 (chloroquine-resistant) with IC_{50} values of 0.87 and 0.39 μM, and 0.90 and 0.43 μM, respectively. Plakortin causes dose and time-dependent morphological anomalies, early maturation delays, reactive oxygen species (ROS) generation, and lipid peroxidation in the parasite	79 and[102]
Fungus	Georatusin (**169**)	*Geomyces auratus*	Georatusin showed antiparasitic activity against *Leishmania donovani* and *Plasmodium falciparum* with IC_{50} values of 9.1 and 1.6 μM	103
Bacteria	Mollemycin A (**170**)	*Streptomyces* sp. (CMB-M0244)	Mollemycin A inhibited 3D7 and Dd2, with IC_{50} values of 9 and 7 nM. Additionally, mollemycin A showed antibacterial activity against *S. aureus* ATCC 25293, *S. aureus* ATCC 9144, *S.* epidermidis ATCC 12228, *B. subtilis* ATCC 6051, and *B. subtilis* ATCC 6633, *Escherichia coli* ATCC 25922, *Pseudomonas aeruginosa* ATCC 27853, with IC_{50} values of 50, 10, 50, 10, 10, 10, and 50 nM	104
Bacteria	Bastimolide A (**171**) and bastimolide B (**172**)	*Okeania hirsute*	Bastimolide A (**171**) and bastimolide B (**172**) inhibited *P. falciparum* HB_3 with IC_{50} values of 2.6 and 5.7 μM	105
Fungus	Polyketide-terpenoid (**173**)	*Peroneutypa* sp. M16	Polyketide-terpenoid (**173**) inhibited 3D7, Dd2, TM90C6B, and 3D7r_MMV848 with IC_{50} values of 19, 37, 19, and 23 μM, respectively	106
Fungus	Canecines A (**174**)	*Penicillium canescens* DJJ-1	Canecines A (**174**) displayed antifungal activity against *C. albicans* with a MIC value of 1 μg mL^{-1}	111
Fungus	Acrophialocinol (**176**) and acrophialocin (**177**)	*Acrophialophora levis*	Acrophialocinol (**176**) and acrophialocin (**177**) inhibited *C. albicans* with MIC values of 25 and 5 μg mL^{-1}, respectively	112
Bacteria	Turonicin A (**178**)	*Streptomyces* sp. MST-123921	It inhibited *Candida albicans* and *Saccharomyces cerevisiae* with MIC values of 0.0031 and 0.0008 μg mL^{-1}. Also, it inhibits *Bacillus subtilis* and *Staphylococcus aureus* with MIC values of 0.097 and 0.39 μ/mL, respectively	113

Chen *et al.* explored the chemical constituents of the *Streptomyces* sp. MST-123921, leading to the identification of the chemical constituent turonicin A. The chemical structure of turonicin A (**178**, Fig. 13) is an amphoteric linear polyene polyketide with independent pentaene and tetraenone chromophores. Turonicin A exhibited potent antifungal activity against *Candida albicans* and *Saccharomyces cerevisiae* and antibacterial activity against *B. subtilis* and *S. aureus*. Notably, turonicin A (**178**) displayed very low toxicity against the NS-1 mouse myeloma cell line, with an IC_{50}, and was inactive against the NFF human fibroblast cell line up to 80 μM. This finding suggests selectivity of turonicin A to pathogens.[113] Potent antimicrobial leads are summarized in Table 2.

6. Conclusions

Numerous microorganisms, particularly bacteria, fungi, and protozoa, play a pivotal role in generating infections that lead to significant mortality and morbidity rates across the globe. Among these, infectious diseases caused by *Mtb* and the ESKAPE pathogens are recognized as leading contributors to health crises, ultimately influencing socio-economic conditions worldwide. While considerable advancements have been made in the medical field, a range of antibiotics has been developed to control and prevent the propagation of infectious diseases. Over recent decades, the emergence of multiple multidrug-resistant pathogens presents considerable challenges in treatment strategies involving conventional antibiotics. This pressing issue underscores the necessity of urgently identifying novel therapeutic molecules that utilize innovative mechanisms of action to tackle pathogens.

Natural products stand out as invaluable resources in the quest for new drugs, offering a remarkable variety of chemical structures, each demonstrating unique complexity and potential therapeutic benefits. This exceptional diversity instills hope for discovering new treatments and emphasizes the critical need to explore these natural compounds in the fight against infectious diseases. An intriguing aspect of this exploration is the polyketide synthase machinery, which is abundantly present in various natural sources such as bacteria, plants, and fungi. This biochemical system is responsible for synthesizing a wide range of chemotypes. Notably, several polyketide-based compounds are used as pharmaceutical agents and have been approved as drugs, showcasing their importance in drug discovery. This work particularly emphasizes the recently identified polyketide-based leads that show promise for treating microbial diseases. These newly discovered molecules have been evaluated in*in vitro* infection models, demonstrating potential applicability in therapeutic scenarios. However, further assessment of these compounds in *in vivo* infection models is essential to validate their therapeutic efficacy and safety.

Author contributions

Gautam Kumar: Data curation, writing original draft, review, and manuscript editing. Sidharth Chopra: Writing, reviewing, and editing the manuscript.

Conflicts of interest

The authors declare no competing interests.

Abbreviations

ACP	Acyl carrier protein
AMR	Antimicrobial resistance
AT	Acyltransferase
DH	Dehydratase
ER	Enoylreductase
ESKAPE	*Enterococcus faecium*, *Staphylococcus aureus*, *Klebsiella pneumoniae*, *Acinetobacter baumannii*, *Pseudomonas aeruginosa*, and *Enterobacter* species
HMG-CoA	3-Hydroxy-3-methylglutaryl-coenzyme A
KR	Ketoreductase
MIC	Minimum inhibitory concentration
MRSA	Methicillin-resistant *Staphylococcus aureus*
Mtb	*Mycobacterium tuberculosis*
PARP1	Poly(ADP-ribose) polymerase-1
PBP	Penicillin-binding protein
PKS	Polyketide synthase
PTP-1B	Protein tyrosine phosphatase-1B
ROS	Reactive oxygen species
TB	Tuberculosis
VRE	Vancomycin-resistant *Enterococcus faecium*
WHO	World Health Organization

Data availability

Since this is a review article, the data can be accessed directly from the manuscript.

Acknowledgements

GK thanks the Director of BITS Pilani for providing the necessary research facilities. This work is supported by the New Faculty Seed Grant (NFSG/PIL/2024/P3862) from the Institute BITS Pilani, Pilani campus.

References

1 E. Alirol, L. Getaz, B. Stoll, F. Chappuis and L. Loutan, *Lancet Infect. Dis.*, 2011, **11**, 131–141.
2 J. M. van Seventer and N. S. Hochberg, in *International Encyclopedia of Public Health*, Elsevier Inc., 2016, pp. 22–39.
3 S. Biswas, H. Khuntia, M. Bal, S. Pati and M. Ranjit, *One Health Bulletin*, 2023, **3**, 20.
4 WHO, *Global Tuberculosis Report*, 2022.
5 S. Fatima, A. Kumari, G. Das and V. P. Dwivedi, *Life Sci.*, 2020, **252**, 1–10.
6 WHO Reports 2023, *Global Tuberculosis Report 2023*, World Health Organization, 2023.

7 WHO, *World Malaria Report 2023*, World Health Organization, 2023.
8 M. L. Rodrigues and J. D. Nosanchuk, *PLoS Neglected Trop. Dis.*, 2020, **14**, 1–9.
9 D. M. P. De Oliveira, B. M. Forde, T. J. Kidd, P. N. A. Harris, M. A. Schembri, S. A. Beatson, D. L. Paterson and M. J. Walker, *Clin. Microbiol. Rev.*, 2020, **33**, 1–49.
10 World Health Organization, *WHO Bacterial Priority Pathogens List, 2024:Bacterial Pathogens of Public Health Importance to Guide Research, Development and Strategies to Prevent and Control Antimicrobial Resistance*, 2024.
11 E. Leung, D. E. Weil, M. Raviglione and H. Nakatani, *Bulletin of the World Health Organization*, 2011, 390–392.
12 J. G. Montoya, K. Laessig, M. S. Fazeli, G. Siliman, S. S. Yoon, E. Drake-Shanahan, C. Zhu, A. Akbary and R. McLeod, *Eur. J. Med. Res.*, 2021, DOI: 10.1186/s40001-021-00606-7.
13 S. Lu, J. Wang, R. Sheng, Y. Fang and R. Guo, *Chem. Biodiversity*, 2020, DOI: 10.1002/cbdv.202000562.
14 C. L. Cazer, E. R. B. Eldermire, G. Lhermie, S. A. Murray, H. M. Scott and Y. T. Gröhn, *Prev. Vet. Med.*, 2020, **176**, DOI: 10.1016/j.prevetmed.2020.104934.
15 J. W. Han, G. J. Choi and B. S. Kim, *World J. Microbiol. Biotechnol.*, 2018, DOI: 10.1007/s11274-018-2546-0.
16 H. Peng, K. Ishida, Y. Sugimoto, H. Jenke-Kodama and C. Hertweck, *Nat. Commun.*, 2019, **10**(1), DOI: 10.1038/s41467-019-11896-1.
17 X. Di, P. Li, Y. Xiahou, H. Wei, S. Zhi and L. Liu, *J. Agric. Food Chem.*, 2024, DOI: 10.1021/acs.jafc.4c03750.
18 A. T. Keatinge-Clay, *Angew. Chem., Int. Ed.*, 2017, **56**, 4658–4660.
19 W. He, W. Wang, J. Ma, G. Zheng, A. A. Zimin, W. Jiang, J. Tian and Y. Lu, *Appl. Microbiol. Biotechnol.*, 2022, **106**, 2147–2159.
20 S. Schulz, H. Sletta, K. Fløgstad Degnes, S. Krysenko, A. Williams, S. M. Olsen, K. Vernstad, A. Mitulski and W. Wohlleben, *Appl. Microbiol. Biotechnol.*, 2023, **107**, 2871–2886.
21 L. Xie, G. Zhu, J. Shang, X. Chen, C. Zhang, X. Ji, Q. Zhang and Y. Wei, *Cell. Signal*, 2021, **87**, DOI: 10.1016/j.cellsig.2021.110122.
22 Z. Xiong, X. Cao, Q. Wen, Z. Chen, Z. Cheng, X. Huang, Y. Zhang, C. Long, Y. Zhang and Z. Huang, *Food Chem. Toxicol.*, 2019, **131**, DOI: 10.1016/j.fct.2019.110585.
23 Y. Liang, Q. Li, M. Wei, C. Chen, W. Sun, L. Gu, H. Zhu and Y. Zhang, *Bioorg. Chem.*, 2020, **99**(1), 8, DOI: 10.1016/j.bioorg.2020.103760.
24 C. Hertweck, *Angew. Chem.*, 2015, **127**, 14830–14832.
25 L. Dong and J. Zhang, *Adv. Agrochem*, 2022, 100–112.
26 R. Laing, V. Gillan and E. Devaney, *Trends Parasitol.*, 2017, 463–472, DOI: 10.1016/j.pt.2017.02.004.
27 J. Zhang, Y. J. Yan, J. An, S. X. Huang, X. J. Wang and W. S. Xiang, *Microb. Cell Fact.*, 2015, **14**(1), 1–12.
28 U. R. Lal and A. Singh, *Stud. Nat. Prod. Chem.*, 2016, **48**, 263–285.
29 K. R. Hardie and S. J. Fenn, *J. Med. Microbiol.*, 2022, **71**(8), 1–5.
30 T. H. Grossman, *Cold Spring Harbor Perspect. Med.*, 2016, **6**(4), 1–24.
31 F. Liu and A. G. Myers, *Curr. Opin. Chem. Biol.*, 2016, 48–57.
32 S. Mawatwal, A. Behura, A. Ghosh, S. Kidwai, A. Mishra, A. Deep, S. Agarwal, S. Saha, R. Singh and R. Dhiman, *Biochim. Biophys. Acta, Gen. Subj.*, 2017, **1861**, 3190–3200.
33 N. P. Ranjan and P. Das, *Biochim. Biophys. Acta, Gen. Subj.*, 2024, **1868**(2), 1–13.
34 S. Khoshnood, M. Heidary, A. Asadi, S. Soleimani, M. Motahar, M. Savari, M. Saki and M. Abdi, *Biomed. Pharmacother.*, 2019, 1809–1818.
35 M. Dadashi, B. Hajikhani, D. Darban-Sarokhalil, A. van Belkum and M. Goudarzi, *J. Global Antimicrob. Resist.*, 2020, 238–247.
36 P. Szczeblewski, T. Laskowski, A. Balka, E. Borowski and S. Milewski, *J. Nat. Prod.*, 2018, **81**, 1540–1545.
37 M. Szomek, P. Reinholdt, D. Petersen, A. Caci, J. Kongsted and D. Wüstner, *Biochim. Biophys. Acta, Biomembr.*, 2021, **1863**(2), 1–11.
38 N. Alomeir, Y. Zeng, A. Fadaak, T. T. Wu, H. Malmstrom and J. Xiao, *Arch. Oral Biol.*, 2023, **145**, 1–9.
39 Y. Bin Bai, Y. Q. Gao, X. Di Nie, T. M. L. Tuong, D. Li and J. M. Gao, *J. Agric. Food Chem.*, 2019, **67**, 6125–6132.
40 P. Buchy, S. Ascioglu, Y. Buisson, S. Datta, M. Nissen, P. A. Tambyah and S. Vong, *Int. J. Infect. Dis.*, 2020, **90**, 188–196.
41 M. F. Varela, J. Stephen, M. Lekshmi, M. Ojha, N. Wenzel, L. M. Sanford, A. J. Hernandez, A. Parvathi and S. H. Kumar, *Antibiotics*, 2021, **10**(5), 1–22.
42 G. Kumar and A. Kiran Tudu, *Bioorg. Med. Chem.*, 2023, **80**, 1–20.
43 G. Kumar, *RSC Med. Chem.*, 2025, **16**, 561–604.
44 K. Chakraborty, V. K. Kizhakkekalam and M. Joy, *Phytochemistry*, 2022, **193**, 1–13.
45 K. A. Uz Zaman, A. M. Sarotti, X. Wu and S. Cao, *Phytochemistry*, 2022, **198**, 1–8.
46 I. A. Osterman, M. Wieland, T. P. Maviza, K. A. Lashkevich, D. A. Lukianov, E. S. Komarova, Y. V. Zakalyukina, R. Buschauer, D. I. Shiriaev, S. A. Leyn, J. E. Zlamal, M. V. Biryukov, D. A. Skvortsov, V. N. Tashlitsky, V. I. Polshakov, J. Cheng, Y. S. Polikanov, A. A. Bogdanov, A. L. Osterman, S. E. Dmitriev, R. Beckmann, O. A. Dontsova, D. N. Wilson and P. V. Sergiev, *Nat. Chem. Biol.*, 2020, **16**, 1071–1077.
47 V. A. Alferova, T. P. Maviza, M. V. Biryukov, Y. V. Zakalyukina, V. I. Polshakov, P. V. Sergiev, V. A. Korshun and I. A. Osterman, *Biochimie*, 2023, **206**, 150–153.
48 Y. F. Yan, Y. Liu, H. Liang, L. Cai, X. Y. Yang and T. P. Yin, *J Proteomics*, 2024, **292**, 1–9.
49 C. D. Fage, T. Lathouwers, M. Vanmeert, L. J. Gao, K. Vrancken, E. M. Lammens, A. N. M. Weir, R. Degroote, H. Cuppens, S. Kosol, T. J. Simpson, M. P. Crump, C. L. Willis, P. Herdewijn, E. Lescrinier, R. Lavigne, J. Anné and J. Masschelein, *Angew. Chem., Int. Ed.*, 2020, **59**, 10549–10556.

50 P. D. Walker, C. Williams, A. N. M. Weir, L. Wang, J. Crosby, P. R. Race, T. J. Simpson, C. L. Willis and M. P. Crump, *Angew. Chem., Int. Ed.*, 2019, **58**, 12446–12450.
51 A. Hoffmann, U. Steffens, B. Maček, M. Franz-Wachtel, K. Nieselt, T. A. Harbig, K. Scherlach, C. Hertweck, H.-G. Sahl and G. Bierbaum, *mSphere*, 2024, **9**(5), 1–21.
52 P. Hou, V. H. Woolner, J. Bracegirdle, P. Hunt, R. A. Keyzers and J. G. Owen, *J. Nat. Prod.*, 2023, **86**, 526–532.
53 X. Jian, F. Pang, C. Hobson, M. Jenner, L. M. Alkhalaf and G. L. Challis, *J. Am. Chem. Soc.*, 2024, **146**, 6114–6124.
54 N. L. Heath, R. S. Rowlands, G. Webster, E. Mahenthiralingam and M. L. Beeton, *J. Appl. Microbiol.*, 2021, **130**, 1546–1551.
55 Y. D. Petrova and E. Mahenthiralingam, *Cell Surf.*, 2022, **8**, 1–6.
56 C. Simm, T. H. Lee, H. Weerasinghe, D. Walsh, I. T. Nakou, M. Shankar, W. C. Tse, Y. Zhang, R. Inman, R. J. Mulder, F. Harrison, M. I. Aguilar, G. L. Challis and A. Traven, *mBio*, 2024, **15**, e0261124.
57 G. Kumar and K. Engle, *Nat. Prod. Rep.*, 2023, 1608–1646.
58 Z. Liu, Y. Yashiroda, P. Sun, H. Ma, Y. Wang, L. Li, F. Yan and Y. Sun, *Org. Lett.*, 2023, **25**, 571–575.
59 N. Tanabe, R. Takasu, Y. Hirose, Y. Kamei, M. Kondo and A. Nakabachi, *Microbiol. Spectrum*, 2022, **10**(4), 1–15.
60 K. Chakraborty, V. K. Kizhakkekalam, M. Joy and S. Dhara, *Appl. Microbiol. Biotechnol.*, 2021, DOI: **10.1007/s00253-021-11390-z**.
61 K. Chakraborty, V. K. Kizhakkekalam, M. Joy and R. D. Chakraborty, *Appl. Microbiol. Biotechnol.*, 2022, **106**, 329–340.
62 P. Vrabl, B. Siewert, J. Winkler, H. Schöbel, C. W. Schinagl, L. Knabl, D. Orth-Höller, J. Fiala, M. S. Meijer, S. Bonnet and W. Burgstaller, *Microb. Cell Fact.*, 2022, **21**(1), 1–16.
63 T. Kimura, M. Umekita, M. Hatano, C. Hayashi, R. Sawa and M. Igarashi, *J. Antibiot.*, 2022, **75**, 535–541.
64 B. Kepplinger, L. Mardiana, J. Cowell, S. Morton-Laing, Y. Dashti, C. Wills, E. C. L. Marrs, J. D. Perry, J. Gray, M. Goodfellow, J. Errington, M. R. Probert, W. Clegg, J. Bogaerts, W. Herrebout, N. E. E. Allenby and M. J. Hall, *Sci. Rep.*, 2022, **12**(1), 1–11.
65 T. Wu, A. A. Salim, Z. G. Khalil, P. V. Bernhardt and R. J. Capon, *J. Nat. Prod.*, 2022, **85**, 1641–1657.
66 T. X. Li, H. H. Dong, L. Xing, L. He, R. Y. Zhang, D. Y. Shao, Y. X. Dai, D. L. Li and C. P. Xu, *Fitoterapia*, 2024, **173**, 1–6.
67 Y. Yang, G. D. Li, Y. T. Shao, Z. W. Sun, L. W. Li, W. Li and H. T. Li, *Fitoterapia*, 2024, **173**, 1–5.
68 K. Chakraborty, V. K. Kizhakkekalam and M. Joy, *Bioorg. Chem.*, 2021, **108**(1), 1–12.
69 Z. Wang, X. He, C. Niu, J. Zhou and Z. Zhang, *Phytochem. Lett.*, 2022, **47**, 42–45.
70 H. Zhang, C. P. Li, L. L. Wang, Z. Da Zhou, W. Sen Li, L. Y. Kong and M. H. Yang, *Chin. Chem. Lett.*, 2024, **35**(9), 1–4.
71 P. Zhao, M. Yang, G. Zhu, B. Zhao, H. Wang, H. Liu, X. Wang, J. Qi, X. Yin, L. Yu, Y. Meng, Z. Li, L. Zhang and X. Xia, *J. Antibiot.*, 2021, **74**, 317–323.
72 Z. Qin, J. T. Munnoch, R. Devine, N. A. Holmes, R. F. Seipke, K. A. Wilkinson, B. Wilkinson and M. I. Hutchings, *Chem. Sci.*, 2017, **8**, 3218–3227.
73 J. Yuan, L. Wang, J. Ren, J. P. Huang, M. Yu, J. Tang, Y. Yan, J. Yang and S. X. Huang, *J. Nat. Prod.*, 2020, **83**, 1919–1924.
74 L. Yang, X. Li, P. Wu, J. Xue, L. Xu, H. Li and X. Wei, *J. Antibiot.*, 2020, **73**, 283–289.
75 X. Li, P. Wu, H. Li, J. Xue, H. Xu and X. Wei, *J. Nat. Prod.*, 2021, 1806–1815.
76 H. X. Yang, J. T. Ma, J. He, Z. H. Li, R. Huang, T. Feng and J. K. Liu, *ACS Omega*, 2021, **6**, 25089–25095.
77 S. Chen, C. Zhang and L. Zhang, *Angew. Chem., Int. Ed.*, 2022, **61**(24), 1–9.
78 V. C. Fäseke, F. C. Raps and C. Sparr, *Angew. Chem.*, 2020, **132**, 7039–7047.
79 R. Orfali, S. Perveen, A. Al-Taweel, A. F. Ahmed, N. Majrashi, K. Alluhay, A. Khan, P. Luciano and O. Taglialatela-Scafati, *J. Nat. Prod.*, 2020, **83**, 3591–3597.
80 F. Maglangit, S. Wang, A. Moser, K. Kyeremeh, L. Trembleau, Y. Zhou, D. J. Clark, J. Tabudravu and H. Deng, *J. Nat. Prod.*, 2024, **87**, 831–836.
81 F. Pan, D. H. El-Kashef, R. Kalscheuer, W. E. G. Müller, J. Lee, M. Feldbrügge, A. Mándi, T. Kurtán, Z. Liu, W. Wu and P. Proksch, *Eur. J. Med. Chem.*, 2020, **191**, 1–7.
82 Y. F. Liu, Y. H. Zhang, C. L. Shao, F. Cao and C. Y. Wang, *J. Nat. Prod.*, 2020, **83**, 1300–1304.
83 K. Chakraborty, B. Thilakan and V. K. Raola, *Phytochemistry*, 2017, **142**, 112–125.
84 K. Chakraborty, B. Thilakan, V. K. Raola and M. Joy, *Food Chem.*, 2017, **218**, 427–434.
85 V. K. Kizhakkekalam, K. Chakraborty and M. Joy, *Int. J. Antimicrob. Agents*, 2020, **55**(3), 1–11.
86 K. Ishida, G. Shabuer, S. Schieferdecker, S. J. Pidot, T. P. Stinear, U. Knuepfer, M. Cyrulies and C. Hertweck, *Chem.—Eur. J.*, 2020, **26**, 13147–13151.
87 B. Kepplinger, S. Morton-Laing, K. H. Seistrup, E. C. L. Marrs, A. P. Hopkins, J. D. Perry, H. Strahl, M. J. Hall, J. Errington and N. E. Ellis Allenby, *ACS Chem. Biol.*, 2018, **13**, 207–214.
88 L. Sun, H. Zhu, L. Zhang, Y. Zhu, D. Ratnasekera, C. Zhang and Q. Zhang, *J. Nat. Prod.*, 2023, **86**, 979–985.
89 Z. G. Khalil, A. A. Salim, D. Vuong, A. Crombie, E. Lacey, A. Blumenthal and R. J. Capon, *J. Antibiot.*, 2017, **70**, 1097–1103.
90 S. T. Bo, Z. F. Xu, L. Yang, P. Cheng, R. X. Tan, R. H. Jiao and H. M. Ge, *J. Antibiot.*, 2018, **71**, 601–605.
91 W. H. Liu, Y. Ding, X. Ji, F. L. An and Y. H. Lu, *J. Antibiot.*, 2019, **72**, 111–113.
92 Y. P. Luo, C. J. Zheng, G. Y. Chen, X. P. Song and Z. Wang, *J. Antibiot.*, 2019, **72**, 513–517.
93 L. Boudesocque-Delaye, D. Agostinho, C. Bodet, I. Thery-Kone, H. Allouchi, A. Gueiffier, J. M. Nuzillard and C. Enguehard-Gueiffier, *J. Nat. Prod.*, 2015, **78**, 597–603.
94 J. B. Jouda, I. K. Mawabo, A. Notedji, C. D. Mbazoa, J. Nkenfou, J. Wandji and C. N. Nkenfou, *Int. J. Mycobact.*, 2016, **5**, 192–196.

95 X. Xia, S. Kim, S. Bang, H. J. Lee, C. Liu, C. Il Park and S. H. Shim, *J. Antibiot.*, 2015, **68**, 139–141.
96 W. Guo, Z. Zhang, T. Zhu, Q. Gu and D. Li, *J. Nat. Prod.*, 2015, **78**, 2699–2703.
97 M. Mushtaque and Shahjahan, *J. Med. Chem.*, 2015, 280–295.
98 A. Chugh, A. Kumar, A. Verma, S. Kumar and P. Kumar, *Med. Chem. Res.*, 2020, 1723–1750.
99 P. N. Kalaria, S. C. Karad and D. K. Raval, *Eur. J. Med. Chem.*, 2018, 917–936.
100 A. Kantele and T. S. Jokiranta, *Clin. Infect. Dis.*, 2011, **52**, 1356–1362.
101 G. Chianese, M. Persico, F. Yang, H. W. Lin, Y. W. Guo, N. Basilico, S. Parapini, D. Taramelli, O. Taglialatela-Scafati and C. Fattorusso, *Bioorg. Med. Chem.*, 2014, **22**, 4572–4580.
102 O. A. Skorokhod, D. Davalos-Schafler, V. Gallo, E. Valente, D. Ulliers, A. Notarpietro, G. Mandili, F. Novelli, M. Persico, O. Taglialatela-Scafati, P. Arese and E. Schwarzer, *Free Radical Biol. Med.*, 2015, **89**, 624–637.
103 Y. M. Shi, C. Richter, V. L. Challinor, P. Grün, A. Girela Del Rio, M. Kaiser, A. Schüffler, M. Piepenbring, H. Schwalbe and H. B. Bode, *Org. Lett.*, 2018, **20**, 1563–1567.
104 R. Raju, Z. G. Khalil, A. M. Piggott, A. Blumenthal, D. L. Gardiner, T. S. Skinner-Adams and R. J. Capon, *Org. Lett.*, 2014, **16**, 1716–1719.
105 C. L. Shao, X. F. Mou, F. Cao, C. Spadafora, E. Glukhov, L. Gerwick, C. Y. Wang and W. H. Gerwick, *J. Nat. Prod.*, 2018, **81**, 211–215.
106 M. R. de Amorim, C. de S. Barbosa, T. A. Paz, L. P. Ióca, K. J. Nicácio, L. F. P. de Oliveira, M. O. Goulart, J. M. Paulino, M. O. da Cruz, A. G. Ferreira, M. Furlan, S. P. de Lira, R. A. dos Santos, A. Rodrigues, R. V. C. Guido and R. G. S. Berlinck, *J. Nat. Prod.*, 2023, **86**, 1476–1486.
107 A. Casadevall, *Pathog. Immun.*, 2018, **3**, 183.
108 N. Liu, J. Tu, G. Dong, Y. Wang and C. Sheng, *J. Med. Chem.*, 2018, **61**, 5484–5511.
109 D. Z. P. Friedman and I. S. Schwartz, *J. Fungi*, 2019, **5**(3), 1–19.
110 J. Song, J. Zhou, L. Zhang and R. Li, *Microorganisms*, 2020, **8**, 1–15.
111 J. P. Wang, Y. Shu, S. Q. Zhang, L. L. Yao, B. X. Li, L. Zhu, X. Zhang, H. Xiao, L. Cai and Z. T. Ding, *Phytochemistry*, 2023, **206**, 1–7.
112 C. Wieder, M. Künzer, R. Wiechert, K. Seipp, K. Andresen, P. Stark, A. Schüffler, T. Opatz and E. Thines, *Org. Lett.*, 2025, **27**, 1036–1041.
113 R. Chen, S. A. Minns, J. A. Kalaitzis, M. S. Butler, M. Rosin, D. Vuong, S. S. Lean, Y. H. Chooi, E. Lacey and A. M. Piggott, *J. Nat. Prod.*, 2023, **86**, 2054–2058.